Population genetic dynamics of Himalayan-Hengduan tree peonies, *Paeonia* subsect. *Delavayanae*

Jin-Mei Zhang[a, b*], Jordi López-Pujol[c*§], Xun Gong[d], Hua-Feng Wang[a, e], Roser Vilatersana[c] and Shi-Liang Zhou[a§]

[a]State Key Laboratory of Systematic and Evolutionary Botany, Institute of Botany, Chinese Academy of Sciences, Nanxincun 20, Xiangshan, 100093 Beijing, China

[b]National Genebank, Institute of Crop Science (ICS), Chinese Academy of Agricultural Sciences (CAAS), Nan Dajie 12, Zhongguancun, Beijing 100081, China

[c]Botanic Institute of Barcelona (IBB, CSIC-ICUB), Passeig del Migdia s/n, 08038 Barcelona, Spain

[d]Kunming Institute of Botany, Chinese Academy of Sciences, Kunming 650204, China

[e]Hainan Key Laboratory for Sustainable Utilization of Tropical Bioresources, Institute of Tropical Agriculture and Forestry, Hainan University, Haikou 570228, China

*These authors contributed equally to this work

[§]Corresponding authors email: jlopez@ibb.csic.com; slzhou@ibcas.ac.cn

Running head: **Population genetics of *Paeonia* subsect. *Delavayanae***

Abstract

According to the present taxonomical treatment, *Paeonia* subsect. *Delavayanae* consists of only two species (*P. delavayi* and *P. ludlowii*) endemic to the Himalayan-Hengduan Mountains. Although *P. ludlowii* can be distinguished from *P. delavayi* on the basis of a series of morphological characters, the species delimitation remains controversial because the more widespread one, *P. delavayi*, exhibits considerable morphological diversity. Both chloroplast DNA markers and nuclear microsatellites or simple sequence repeats (nSSR) are used herein to reveal genetic diversity and relationships of the two taxa included in this subsection, and ecological niche modeling (ENM) is employed to get insights into their paleodistribution. Our results show that genetic boundaries between the two currently recognized species are unclear, probably due to recent divergence. *Paeonia ludlowii* is budding from *P. delavayi*, probably by genetic isolation but also by shifting its niche to the harsher upland Tibetan conditions. *Paeonia delavayi* itself would be, however, under active speciation, showing significant genetic differentiation and morphological diversity. Whereas *P. ludlowii* would have endured the Pleistocene glacial periods by *in situ* persistence in local, small refugia, a 'dual' model seems to apply for *P. delavayi* (*in situ* persistence and retreat to refugia). The rarity of *P. ludlowii* and high evolutionary potential of *P. delavayi* imply high priority of *in situ* conservation of both taxa. The Himalayan-Hengduan Mountains are an ideal arena for differentiation within subsect. *Delavayanae* of *Paeonia*, by means of expansions/contractions/displacements, vertical migration, and local survival/extinctions in response to the Neogene climate fluctuations and geological changes.

Keywords: biogeography; conservation; genetic diversity; *Paeonia*; differentiation.

1. Introduction

Mountain ranges are regarded as one of the most important drivers of plant evolutionary divergence and speciation, both in the tropics and in temperate regions (Hugues and Atchison, 2015; Schwery et al., 2015). The formation and the complex orography of mountains, often coupled with large climatic changes, shaped the historical population demography and genetic diversity generally by strong selection, quick genetic drift and limited gene flow. As a consequence, mountains are generally associated with high levels of plant diversity, both in terms of species richness and endemism (e.g., Barthlott et al., 2005). The Qinghai-Tibetan Plateau (QTP), the highest (with an average elevation exceeding 4500 m) and one of the largest plateaus of the world (with about 2.5 million km^2), is one of the regions with most active plant evolution (Liu et al., 2014; Wen et al., 2014; Favre et al., 2015; Xing and Ree, 2017), largely due to its active tectonism (with major uplift events commencing 40 Ma and continuing at present; Mulch and Camberlain, 2006), large altitudinal gradients (from 500 m at the foot of the Himalayas to the 8848 m of the Mt. Everest), and the enormous diversity of habitats and climatic conditions (e.g., the annual precipitation may vary from 100 mm to about 3000 mm; Favre et al., 2015). However, most speciation events happened in the southernmost part, the Himalayas and the Hengduan Mountains, which are recognized as two of the 25 global biodiversity hotspots. It is estimated that there are around 10,000 species (with 3160 endemisms) in the Himalayas, and ca. 12,000 species (with 3500 endemisms) in the Hengduan Mountains (Mittermeier et al., 2011). The division of Himalayas and Hengduan Moutains is somewhat arbitrary, and indeed many species occur in both regions, which are increasingly referred to as 'Himalayan-Hengduan Mountains (HHM)' (e.g., Luo et al., 2016).

The HHM is an arena for active plant radiation and speciation in the world due to the combination of continued mountain uplift, a very complex topography (the Hengduan Mountains are probably the most rugged ones on Earth), and Quaternary climatic oscillations. In response to these factors, plants have diversified through multiple mechanisms that include allopatric speciation, hybridization, polyploidy, ecological adaptation, and even morphological innovations. Mountain uplift is certainly the main trigger for some of the best-known HHM rapid radiations (e.g., *Aconitum* L./*Delphinium* L., *Pedicularis* L., *Rhododendron* L., *Saussurea* DC., or the *Ligularia* Cass./*Cremanthodium* Benth./*Parasenecio* W.W. Sm. & J. Small complex; Wen et al., 2014; Hugues and Atchison, 2015), and also for intraspecific differentiation in some plant species [e.g., *Hippophae tibetana* Schltdl., *Meconopsis integrifolia* (Maxim.) Franch., and *Taxus wallichiana* Zucc.; Wang et al., 2010; Yang et al., 2012; Liu et al., 2013], given that uplift would have been active until Pliocene and Pleistocene (Li and Fang, 1999; Favre et al., 2015). Nevertheless, the main triggers that mostly delineated the intraspecific genetic and phylogeographic structure of HHM plants were the Quaternary climatic oscillations coupled with the very complex regional topography. Although the QTP was not covered by a large ice sheet (such as the Laurentide one), glaciers and ice caps occupied large parts (about 350,000 km^2; Shi, 2002), especially in the Himalayas. In contrast, the Hengduan Mountains, particularly their southern section, remained relatively ice-free (Li et al., 1991; Shi, 2002), likely having served as a refugium. The expectation of range shifts from the Himalayas (or other parts of the QTP) to large glacial refugia located in the Hengduan Mountains during glacial periods (followed by postglacial recolonizations) is however, not always met; many HHM plant species, especially those cold-tolerant, instead of migrating into these (warm) refugia, would have

survived *in situ* in small refugia (Qiu et al., 2011; Liu et al., 2014; Luo et al., 2016).

Paeoniaceae is a small family of only one genus, *Paeonia* L., and ca. 33 species, distributed in the northwestern corner of Africa, Europe, Asia and western North America (Hong, 2010). The genus has diverged into woody (sect. *Moutan* DC., commonly known as 'tree peony' and *mudan* in Chinese) as well as herbaceous forms (sect. *Paeonia* and sect. *Onaepia* Lindl.). The tree peony is crowned 'the king of flowers' in China for its beauty. It first appeared in royal gardens during the Tang dynasty (618–907 AD) or earlier, and today it is extensively cultivated in China for medicinal and oil uses. About 1000 ornamental cultivars have been created in China alone (He and Xing, 2015). The section *Moutan* contains nine diploid ($2n$ = 10) species endemic to China and is subdivided into two subsections, *Delavayanae* Stern and *Vaginatae* Stern (Hong, 2010). The subsect. *Delavayanae* consists of only two species (Hong, 2010). One is *P. delavayi* Franch., restricted to sparse thickets, woods or forests in southeastern Tibet, northern Yunnan and western Sichuan provinces at altitudes of 1900–4000 m (Fig. 1A). The other is *P. ludlowii* (Stern & G. Taylor) D.Y. Hong, which is endemic to a small area in three counties (Lhünzê, Mainling, Nyingchi) of southeastern Tibet (Fig. 1A).

The taxonomy of subsect. *Delavayanae* has been controversial because the type species, *P. delavayi*, exhibits considerable morphological diversity in the width of leaf segments and the number, size, and color of floral parts (Hong et al., 1998). A plethora of names at specific or varietal ranks was given to morphoforms; for example, *P. delavayi* for the dark red flower form, *P. lutea* Delavay ex Franch. for the yellow flower form, *P. potaninii* Komarov for the finely lobed form, *P. trollioides* Stapf ex Stern for the yellowish pink or pinkish yellow flower form, and *P. weisiensis* Y. Wang & K. Li for the white or pale yellow flower form. All these names have been synonymized under *P. delavayi* with the exception of *P. lutea* var. *ludlowii* Stern & G. Taylor, which was upgraded to the species rank (*P. ludlowii*) on the basis of a series of morphological characters (single carpels, larger follicles, yellow petals, and lack of stolons (Hong, 1997, 2010; Hong et al., 1998). Such two-species taxonomic treatment for subsect. *Delavayanae* was supported by recent molecular evidence (Zhang et al., 2009a; Zhou et al., 2014).

It is expected that, being dwellers in HHM region, *P. delavayi* and *P. ludlowii* would have experienced range expansions/contractions, vertical migration, displacements, and local survival/extinctions in given refugia as consequence of the Neogene climate fluctuations and mountain building processes, leaving some imprints on their geographical patterns. In this study, we will use maternally-inherited plastid DNA sequences and nuclear microsatellites or simple sequence repeats (nSSR), as well as ecological niche modeling (ENM), to unravel the population dynamics of the HHM tree peonies (*P. delavayi* and *P. ludlowii*). ENM is often employed to get insights into the paleodistribution of species, being an ideal complement to genetic markers (Huang and Schaal, 2012). More specifically, we aimed to: (1) evaluate the phylogenetic and relationships between *P. delavayi* and *P. ludlowii*; (2) reconstruct the phylogeographic relationships among populations of both species; (3) estimate the levels of intrapopulation genetic diversity, as well as the interpopulation genetic and phylogeographic structure; (4) reveal the effects of complex landforms, the Quaternary climatic oscillations (including the formation of ice-caps), and the last phases of mountain uplift on the genetic and phylogeographic patterns; and (5) estimate the potential distribution both at present and in the

past and determine whether there is niche conservatism or niche divergence between the two species.

Data obtained in this study will shed light on the HHM tree peony diversification; such information would be especially relevant for their conservation, as both *P. delavayi* and *P. ludlowii* have been traditionally harvested for both horticultural (Zhang et al., 2011) and medicinal (Hong, 2010; Yang et al., 2014) purposes. Although only *P. ludlowii* is considered threatened (it is listed as 'endangered' in 2013 version of China's IUCN red list; MEP–CAS, 2013), only *P. delavayi* is, ironically, legally protected in China at national level (it is listed as 'third grade' in the *National List of Rare and Endangered Plant Species* of 1984 under the old name *P. delavayi* var. *lutea*). In addition, large parts of *P. delavayi*'s range (especially NW Yunnan) are becoming major touristic hotspots of China.

2. Material and Methods

2.1. Plant material and population sampling

A total of 17 wild populations of subsect. *Delavayanae* (13 populations of *P. delavayi* and four populations of *P. ludlowii*) were sampled in the whole distribution area during the flowering seasons from 1999 to 2006 (Tables 1 and S1). The number of sampled individuals within each population ranged from two in small Tibetan populations to 15 individuals depending on the number of patches and total size of studied populations. Since for *P. delavayi* one patch usually consists of ramets of the same genet, only one sample per patch was collected. For the plastid DNA phylogenetic analysis (see below), we used *P. jishanensis* T. Hong & W. Z. Zhao, *P. ostii* T. Hong & J. X. Zhang. and *P. qiui* Y. L. Pei & D. Y. Hong as outgroups following Zhou et al. (2014). Voucher specimens were deposited in the PE herbarium. Young leaves once collected were quickly dried in silica gel.

2.2. DNA isolation, plastid DNA sequencing and microsatellite genotyping

Total genomic DNA was extracted from silica gel-dried leaves according to the mCTAB method (Li et al., 2013). After preliminarily screening of seven chloroplast loci, the most variable ones (*ndh*C-*trn*V$^{(UAC)}$, *ndh*F, *psb*A-*trn*H, and *rps*16-*trn*Q) were finally selected as markers for this study. The primers used and detailed PCR profiles are given in Table S2. Polyethylene glycol (PEG8000) was used for purifying the PCR products. The fragments were sequenced on an AB 3730*xl* DNA analyzer (Applied Biosystems Inc., Foster City, CA) using both forward and reverse primers. Chloroplast sequences were further edited and assembled using Sequencher v.4.6 (Gene Codes Corporation, Ann Arbor, MI) and adjusted manually. The sequences were submitted to GenBank under accession numbers XXXXX–XXXXX (Table S1).

Each individual was genotyped at nine nSSR loci using the primer pairs designed by Wang et al. (2009) and Zhang et al. (2011) (see Table S3). The 5' ends of the reverse primers were labeled with one of the four fluorescent dyes (FAM, JOE, PET, or NED). The PCR products labeled with different dyes were mixed together in equal ratio and 2.0 μL of the mixture was combined with 7.7 μL of Hi-Di formamide and 0.3 μL of an internal size standard, GeneScan 600LIZ (Applied Biosystems Inc). The fragments were resolved on an AB 3730*xl* DNA Analyzer (Applied Biosystems Inc). Fragment length in base pairs was calculated by GeneMapper v.4.0 (Applied Biosystems Inc).

2.3. Genetic data analysis

2.3.1. Estimation of genetic diversity

Genetic diversity was quantified based on both plastid DNA and nSSR data. Polymorphic sites (S), number of unique haplotypes (h), haplotype diversity (H_d), nucleotide diversity (π) and average number of nucleotide difference (k) were computed with DnaSP v.5.10.01 (Librado and Rozas, 2009) using the combined plastid DNA sequence data. For the nSSR dataset, percentage of polymorphic loci when the most common allele had a frequency of < 0.99 (P_{99}), mean number of alleles per locus (A), observed heterozygosity (H_o), and unbiased expected heterozygosity or Nei's (1978) gene diversity (H_e) were calculated using GenAlEx v.6.5 (Peakall and Smouse, 2006). Allelic richness (AR; rarefacted to compensate for unequal sample sizes; Hurlbert, 1971) was computed with FSTAT v.2.9.3 (Goudet, 1995).

Linkage disequilibrium between pairs of nSSR loci in each population was assessed using FSTAT with significance determined using the Bonferroni correction (Rice, 1989). The frequency of null alleles was estimated following the expectation maximization (EM) algorithm of Dempster et al. (1977) using FreeNA (Chapuis and Estoup, 2007). To test whether populations were under Hardy-Weinberg equilibrium, Wright's (1965) F_{IS} was estimated using nSSR data following the method of Weir and Cockerham (1984) with Genetix v.4.05 (Belkhir et al., 1996–2004). Statistical significance of F_{IS} values for each locus per population was tested by permutation tests (10,000 randomizations), using the same program. Mean F_{IS} was calculated by jackknifing over loci, with bootstrapping to obtain the 95% confidence interval.

2.3.2. Phylogeographic and population structure analyses

Genetic relationships between haplotypes using concatenated sequences were depicted by a statistical parsimony network using TCS v.1.21 (Clement et al., 2000). The highly variable polyT, polyA, polyG, or polyC motifs in the sequences were excluded from the analysis, and indels longer than 1 bp were shortened to single base pair gaps and treated as a fifth character state.

Phylogenetic relationships among haplotypes were reconstructed using Bayesian inference (BI) with MrBayes v.3.1.2. (Ronquist and Huelsenbeck, 2003) and maximum parsimony (MP) method with PAUP v.4.0a149 (Swofford, 2002) by treating gaps as missing values. The best-fit model of substitution for each region was selected by means of jModelTest v.0.1.1 (Posada, 2008) for BI analyses. Bayesian analyses were initiated with random starting trees and four Markov chains were run simultaneously for 10^6 generations and sampled every 100 generations. The first 25% of the runs were discarded as burn-in. The 50% majority rule consensus tree and posterior probabilities (PPs) of the nodes were calculated from the remaining trees. Nodes with PPs ≥ 0.95 were considered to be statistically supported. MP analyses were conducted by heuristic searches with 10,000 replicates with random taxon addition. Bootstrap support (BS) values were generated from 1000 replicates using simple heuristic search algorithm with random sequence addition and TBR branch swapping. Parsimony-uninformative characters were excluded from analysis. BS support ≥ 70% was considered significant.

Pairwise genetic distance between populations based on nSSR dataset was calculated using two algorithms, Nei's (1972) standard genetic distance (D_S) and Rogers' (1972) distance (D_R). These distance matrices were converted into UPGMA (unweighted pair-group method using

arithmetic averages) dendrograms (after 1000 bootstrap replicates) employing the programs Populations v.1.2.30 (Langella, 1999) and TreeView v.1.6 (Page, 1996). A principal coordinate analysis (PCoA), based on codominant genotypic distances, was also conducted using GenAlEx.

Population genetic structure was investigated with both markers using different approaches. First, analysis of molecular variance (AMOVA) was used to examine the distribution of the variance components of genetic diversity within and among populations, based on the complete sample set and several nested analyses. These analyses were performed with Arlequin v.3.5.1.2 (Excoffier and Lischer, 2010) for plastid DNA data and with GenAlEx for nSSRs. Second, the Bayesian algorithm implemented in Structure v.2.3.4 (Pritchard et al., 2000) was used with nSSR dataset. The admixture ancestry model with correlated allele frequencies was selected as the most appropriate option for the analysis. The burn-in period and Markov chain Monte Carlo (MCMC) were set to 50,000 and 500,000 iterations, respectively, and 20 replicates per K were run. The most likely value of K was determined by the ΔK statistic of Evanno et al. (2005), with the aid of Structure Harvester v.0.6.94 (Earl and vonHoldt, 2012). As the ΔK method tends to identify $K = 2$ as the top level of hierarchical structure (Janes et al., 2017), it was combined with the method of choosing the smallest K after the log probability of data [ln Pr($X|K$)] values reached a plateau (Pritchard et al., 2010). Programs Clumpp v.1.1.2 (Jakobsson and Rosenberg, 2007) and Distruct v.1.1 (Rosenberg, 2004) were used to combine the results of the 20 replicates of the best K and to to graphically display the results produced by Clumpp, respectively. And third, Permut v.1.0 (Pons and Petit, 1996) was used with plastid DNA dataset for checking the occurrence of significant phylogeographical structure by testing if G_{ST} (which only takes into account the allele frequencies) and N_{ST} (which uses the distance between different alleles) were significantly different using 10,000 permutations.

The location of potential genetic barriers between populations was explored from both plastid DNA and nSSR datasets through the Monmonier's maximum-difference algorithm implemented in Barrier v.2.2 (Manni et al., 2004). The significance of barriers was tested for nSSR data by bootstraping 1000 Nei's genetic distances D_A (Nei et al., 1983) matrices that were previously obtained with Microsatellite Analyzer (MSA) v.4.05 (Dieringer and Schlötterer, 2003).

To test isolation-by-distance among populations, we estimated Wright's (1965) F_{ST} based on nSSR loci following the method of Weir and Cockerham (1984) and Rousset (1997). Statistical significance of all pairwise F_{ST} values was estimated with Genetix by permutation tests (10,000 randomizations), whereas mean F_{ST} was calculated by jackknifing over loci, with bootstrapping to obtain the 95% confidence interval. The correlation between the matrix of pairwise genetic differentiation [$F_{ST}/(1–F_{ST})$] and the matrix of the log-transformed geographical distances was computed by applying the Mantel test (Mantel, 1967) with 1000 permutations using IBDWS v.3.23 (Jensen et al., 2005).

To reveal recent (i.e., within the last several generations) gene flow between populations, we estimated migration rates based on our nSSR loci using the program BayesAss v.1.3 (Wilson and Rannala, 2003). We ran 3×10^6 MCMC iterations, with a burn-in of 999,999 iterations and a sampling frequency of 2000 by setting delta at 0.15 (the default value).

2.3.3. Population demographical dynamics

In order to detect deviations from the selective neutrality, Tajima's (1989) D, Fu and Li

(1993) F^* and D^*, Fu's (1997) F_S, and Ramos-Onsins and Rozas' (2002) R_2 were computed by using DnaSP. Additionally, using the same software we calculated the mismatch distribution of the pairwise differences between all individuals in a sample to test the population stability or growth (Rogers and Harpending, 1992; Harpending, 1994) and the raggedness index HRI (Harpending, 1994) between observed and expected mismatch distribution as an estimate of the goodness-of-fit. The significance of all the indexes was tested by coalescent analysis using 10,000 replicates.

To test the recent dynamics of effective population size (bottlenecks), we ran the software Bottleneck v.1.2.02 (Piry et al., 1999) using our nSSR dataset for those populations with at least 10 individuals sampled (the minimum requirements of the program). Two different tests were used to check for bottlenecks: the sign test (Cornuet and Luikart, 1996) and the Wilcoxon signed-rank test (Luikart and Cornuet, 1998), both under the infinite allele model (IAM) and the stepwise mutation model (SMM).

2.4. Ecological niche modeling (ENM)

ENM was performed to evaluate the potential distribution of *Paeonia delavayi*, *P. ludlowii*, and *P. delavayi* + *P. ludlowii*. We employed the maximum entropy algorithm, as implemented in MaxEnt v.3.3 (Phillips et al., 2006). The current distribution information for both species was obtained from the sampling sites (Table 1), literature (e.g., Hong, 2010), and specimens deposited in the main Chinese herbaria (www.cvh.ac.cn). After removing duplicate records within each pixel (2.5 arc-min, *ca*. 5 km), we obtained 119 records of *P. delavayi* and 13 records of *P. ludlowii*. A set of 19 bioclimatic variables at 2.5 arc-min resolution covering the distribution range (and neighboring areas) for both species under current conditions (1950–2000) were downloaded from the WorldClim website (www.worldclim.org; Hijmans et al., 2005). Of these, we selected a smaller set of eight relatively uncorrelated ($r \geq |0.9|$) variables (see Supplementary Text 1). The distribution model under current conditions was projected to the Last Glacial Maximum (LGM, ca. 21,000 yr BP) using palaeoclimatic layers simulated by three widely used general circulation models (see Supplementary Text 1). For the cases with a considerable number of occurrences (*P. delavayi* and *P. delavayi* + *P. ludlowii*), 20 replicates of MaxEnt (using the subsample method) were run, and model performance were assessed using the area under the curve (AUC) of the receiver operating characteristic (ROC) plot with 25% of the localities randomly selected to test the model. Given the low number of occurrences for *P. ludlowii* (13), we used a methodology based on a jackknife (or 'leave-one-out') procedure to test the model (Pearson et al., 2007), with the definitive model (i.e., using all occurrence points) running MaxEnt 20 times (using the bootstrap method) (see Supplementary Text 1). The MaxEnt jackknife analysis was used to evaluate the relative importance of the eight bioclimatic variables employed based on their gain values when used in isolation. All ENM predictions were visualized in ArcGIS v.10.2 (ESRI, Redlands, CA, USA).

Niche similarity between *P. delavayi* and *P. ludlowii* was measured through two niche overlap indices, Hellinger-derived *I* and Schoener's *D* as implemented in ENMTools v.1.4.3 (Warren et al., 2010). Two quantitative tests of niche similarity—also implemented in ENMTools—were further used: the 'niche identity test' and the 'background test' (see Supplementary Text 1). For both tests, null distributions were generated from 100 pseudoreplicates. Finally, we estimated the niche breadth for each species by calculating the

inverse concentration statistic of Levins (1968), as implemented in ENMTools.

3. Results

3.1. Genetic diversity

A total of 159 individuals from of *Paeonia* subsect. *Delavayanae* (137 individuals from 13 populations of *P. delavayi* and 22 individuals from four populations of *P. ludlowii*) were sequenced for four loci of chloroplast genome, *ndh*C-*trn*V$^{(UAC)}$, *ndh*F, *psb*A-*trn*H, and *rps*16-*trn*Q. We identified 14 chloroplast haplotypes in *P. delavayi* and one in *P. ludlowii.* Most populations of *P. delavayi* had only one haplotype except DY-LIJ with three haplotypes, and DS-XIA and DY-WEI1 with two different haplotypes; the populations DT-BOM1, DT-BOM2, DT-NYI and DY-DEQ shared the same haplotype (Fig. 1A). At species level, the values of genetic diversity of *P. delavayi* were the following: $H_d = 0.90$, $\pi = 0.19 \times 10^{-2}$, and $k = 4.98$ (see Table S4). No sequence variation was detected in *P. ludlowii*.

With nSSR, 155 individuals from the same 17 populations were genotyped, with all nine surveyed microsatellites being polymorphic across populations. No significant linkage disequilibrium was detected in any of the loci pairs. Only 14 of 90 of all the valid tests showed a significant deviation from Hardy-Weinberg expectations (nine loci showed excess of homozygotes whereas five loci showed excess of heterozygotes), although only one persisted after Bonferroni correction (data not shown). The values of null allele frequency at all loci were very low (all well below 0.100, with a mean of 0.039), indicating that null alleles are not expected to cause significant problems in the analysis (*cf.* Dakin and Avise, 2004; Orsini et al., 2008). In fact, the differences between the 'raw' values of F_{ST} (one of the most sensitive parameters when null alleles occur; Chapuis and Estoup, 2007; Chapuis et al., 2008) and those after correcting for the presence of null alleles in our dataset were absolutely negligible (less than 1%).

A total of 100 alleles were detected and the number of alleles per locus varied greatly among loci, from five (loci *Jx05* and *Pdel11*) to 20 (*Pdel05*), with an average of 11.1 alleles. The values of polymorphism were much higher for populations of *P. delavayi* ($P_{99} = 75.2$, $A = 2.402$, $AR = 1.731$, $H_e = 0.369$) than those of *P. ludlowii* ($P_{99} = 5.6$, $A = 1.056$, $AR = 1.024$, $H_e = 0.013$; Table 2). The most variable populations within the study system were two from NW Yunnan (DY-WEI2 and DY-XIG; Table 2). The four populations of *P. ludlowii* showed extremely low levels of genetic diversity. In fact, three out of four populations were fixed for a single genotype (Table 2). Private alleles were found for most *P. delavayi* populations (ranging from one to six) but were absent in *P. ludlowii* ones (Table 2). Of the 11 alleles occurring in *P. ludlowii*, three were exclusive to this species, whereas the remaining eight were shared with some of the *P. delavayi* populations.

3.2. Phylogeographic and population structure analyses

The rooted TCS network illustrates the relationships among the 15 haplotypes (Fig. 1B). The network shows two large groups of haplotypes, with a weak geographic pattern. The first group included haplotypes H1, H9, H11–H13 and H15, corresponding to Tibetan populations (DT-BOM1, DT-BOM2 and DT-NYI) and Yunnan populations (DY-DEQ, DY-LIJ and DY-WEI1). The second group included haplotypes H2–H8, H10, and H14, corresponding to Yunnan (DY-DAL, DY-KUN, DY-WEI2 and DY-XIG) and Sichuan populations (DS-LIT, DS-MUL

and DS-XIA) and also the four populations of *P. ludlowii*. In the phylogeny of the haplotypes (Fig. 2) we found a similar relationship to the network. The first group was weakly supported (PP = 0.77) and the second group was well supported (PP = 1.00; Fig. 2). The monophyly of *P. delavayi* was not supported by chloroplast data because *P. ludlowii* was nested to the second group. For details of phylogenetic analyses, see Table S5.

With nSSR markers, the UPGMA dendrograms based on Nei's (1972) genetic distance (D_S) and Rogers' (1972) distance (D_R) of nSSR had identical topologies, with the latter one showing somewhat higher bootstrap support at many branches (Figs. 3 and S1). Notably, the Tibetan populations of *P. delavayi* appeared as sister to the rest of populations, whereas *P. ludlowii* was sister to the populations of *P. delavayi* from Sichuan and Yunnan. A similar result was obtained in the PCoA (Fig. 4), with three clearly differentiated groups: *P. ludlowii* populations, the Tibetan populations of *P. delavayi*, and the remaining populations of *P. delavayi.*

The results of the nSSR's AMOVA also confirmed the highly significance and singularity of these three groups of populations (Table 3), as there was a considerable percentage of variance due to differences among these three clusters (38.5%) in nSSR data. However, the among-taxa component only accounted slightly higher, for up to 40.3% (and 42% in plastid DNA) of the total variance.

The results of Structure analyses for all individuals based on the nSSR markers are represented in Figs. 5 and S2. According to Evanno's approach, $K = 2$ and 13 were the most likely numbers of genetic clusters, whereas, when the ln Pr($X|K$) was plotted, the 'plateau' was approximately reached at $K = 11$–13 (Fig. 5). Despite the highest peak for ΔK was at $K = 2$, genetic clustering was highly different between the 20 runs (in only three runs clusters and species coincided; Fig. S3); the two-cluster structure was, therefore, not considered as the most biologically meaningful, although the fact that the four populations of *P. ludlowii* appear together in all runs (Fig. S3) might be of relevance. At $K = 13$, in contrast, a highly stable population structure was found, with 19 of 20 simulations showing the same pattern: each population having its own cluster, with the exception of the four populations of *P. ludlowii* and the three Tibetan populations of *P. delavayi* (each group having its own cluster), and populations DY-LIJ and DY-XIG (these latter showing partial membership to multiple clusters). With the Permut analysis with our plastid DNA dataset, the N_{ST} (0.912 ± 0.054) was not significantly higher than G_{ST} (0.921 ± 0.048), suggesting the absence of phylogeographical structure.

The analysis of genetic barriers based on Monmonier's algorithm with nSSR dataset suggested that strong obstacles to gene flow would exist between Tibetan populations of *P. delavayi* and *P. ludlowii* (Fig. 6A). The first barrier mainly separated Tibetan Nyingchi population (DT-NYI) from the four *P. ludlowii* populations (green barrier, with 93% bootstrap support), whereas the second one separated populations of *P. ludlowii* from the other Tibetan populations of *P. delavayi* (DT-BOMI1 and DT-BOMI2, blue barrier, 90% BS). The third barrier (in red) was weaker (with BS below 80%) and mainly contributed to the separation of most of the populations in the eastern range of *P. delavayi*, as well as DY-DEQ from DT-BOM2 (i.e., the eastern from the western range of *P. delavayi*). The significance of these separations increased with the addition of new barriers, and no additional separations appeared until the 10th barrier was added (Fig. 6A). The genetic barriers revealed by plastid DNA data suggested a relatively different scenario for the eastern populations but not for the western ones (see Fig. 6B).

The genetic differentiation among populations of *P. delavayi* based on F_{ST} was very large [mean F_{ST} (13 populations) = 0.510, 95% CI = 0.451–0.584; see also Table 4]. In contrast, the genetic differentiation between populations of *P. ludlowii* was very low [mean F_{ST} (four populations) = 0.014, 95% CI = -0.002–0.027]. The F_{ST} value between the two species was 0.458. The Mantel test performed for *P. delavayi* revealed a significant positive correlation between genetic and geographic distances ($r^2 = 0.190$, $P = 0.001$).

The BayesAss analysis revealed an almost total absence of recent gene flow between populations. Of the 272 pairwise estimates, only three indicated evidence of recent gene flow between populations: from DS-MUL to DS-XIA ($m = 0.166$), from DY-WEI1 to DS-LIT ($m = 0.223$), and from DY-XIG to DY-LIJ ($m = 0.119$) (Table S6).

3.3. Population demographical dynamics

The mismatch pairwise distance analyses of total plastid DNA dataset (*P. delavayi* + *P. ludlowi*) and at specific level (*P. delavayi*) showed multimodal patterns that suggested dynamical equilibrium (Fig. S4). In addition, no significance was found in any of the studied indexes to detect deviation in the selective neutrality (Table S4). However, DY-LIJ and DY-WEI1 populations showed unimodal mismatch distributions that could be interpreted as these populations have experienced past demographic expansions (Fig. S4).

Bottleneck test results using nSSR data suggested that two populations (DS-MUL, DS-LIT, and DS-XIA) have suffered recent decreases in effective population size (Table 2). However, these results should be taken with extreme caution, as our sample sizes ($N = 10–15$) and number of polymorphic loci (2–9) are below the recommended threshold (20 individuals and 20 loci) to ensure enough statistical power (Cornuet and Luikart, 1996).

3.4. Ecological niche modeling

The AUC scores averaged across 20 runs were very high for both *P. delavayi* and *P. delavayi* + *P. ludlowii* (mean ± SD, 0.937 ± 0.010 and 0.935 ± 0.013, respectively), which supported the predictive power of the model. The model for *P. ludlowii* also performed reasonably well, as we found a high success rate (0.846) and statistical significance ($P < 0.001$) in the jackknife test. According to the MaxEnt jackknife tests of variable importance, the mean temperature of the coldest quarter (bio11) was the most informative for the three models. Although probability maps largely differed among models, there was a general loss of suitable range for both *P. delavayi* and *P. delavayi* + *P. ludlowii* at the LGM when compared to the present (Figs. 7 and S5; Table S7); such loss was mainly focused on southeastern areas (mainly Yunnan) for the MIROC model but on northwestern areas (Tibet and Arunachal Pradesh of India) for the MPI model (Fig. S5). Variability among models was even more evident in *P. ludlowii*, although they should be interpreted with extreme caution given the uncertainty of projecting into the past with a small number of occurrences. The LGM models also indicated a slight decrease in the mean altitude of the suitable habitats compared to the present (Table S7).

Niches of *P. delavayi* and *P. ludlowii* were not identical (Figs. S6A and S6B), although we should take into account that niche identity tests can be seriously biased by the environmental differences that exist between the regions in which two species do not overlap (Warren et al., 2010). While background test overcomes this limitation, results were apparently contradictory: when we compared *P. delavayi* occurrences to *P. ludlowii* background, the observed niche

overlap was significantly larger than the null distribution of niche overlap ($P < 0.05$) for *D* (but not for *I*, which showed no differences; Figs. S6C and S6D). When the test was performed in the inverse direction, observed *I* was significantly smaller than the expected by the null model ($P = 0.00$), while differences were not significant for *D* (Figs. S6E and S6F). Finally, the niche breadth estimate based on ENMs was about five times larger for *P. delavayi* than *P. ludlowii* (0.185 and 0.036, respectively).

4. Discussion

4.1. Relationships between *P. delavayi* and *P. ludlowii* and differentiation within *P. delavayi*

Our genetic data based on nSSR and plastid DNA do not support the current taxonomic treatment of Hong et al. (1998) that *P. delavayi* and *P. ludlowii* are different species. First, the populations of *P. ludlowii* are nested within *P. delavayi* in the UPGMA trees (Figs. 3 and S1); second, the exclusion of $K = 2$ as the best clustering in the Structure analyses (Figs. 5 and S3); and third, phylogenetic tree inferred from plastid DNA indicate that *P. ludlowii* is sister to two Sichuan populations of *P. delavayi*, in a clade placed within a polytomy (Fig. 2). The recent phylogeny of Zhou et al. (2014), which included all the species of section *Moutan* and traditional cultivars, showed that *P. delavayi* and *P. ludlowii* are not distinguishable based on 14 chloroplast regions but, on the contrary, could be delimited based on 25 single-copy nuclear markers. Leaving aside the discrepancy between nuclear and plastid markers (not uncommon in angiosperms; e.g., Zhang et al., 2015), the implications derived from the phylogeny of Zhou et al. (2014) should be treated with caution as only a single individual from a small subset of the extant populations of both *P. delavayi* and *P. ludlowii* were included.

Despite the lack of clear boundaries between *P. delavayi* and *P. ludlowii*, there are some signals of genetic distinctiveness, including the PCoA grouping patterns (*P. ludlowii* appears as a relatively isolated entity; Fig. 4), the Structure clustering patterns (the four populations are clustered together along all surveyed *K* values; Fig S2), and the AMOVA analyses (with the among-taxa component showing a non-negligible value of 40.3%; Table 3). Such results could likely reflect an ongoing differentiation process, apparently following the classical progenitor–derivative (P–D) model of speciation. Under such scenario, D taxon has budded off and acquired new traits (or become fixed for features within the polymorphism of P species) while P species remained largely unchanged (Gottlieb, 2003; Crawford, 2010). In addition to molecular phylogenies (the expected pattern is D taxon to be nested within populations of the P species; Crawford, 2010, see above), morphological traits, allelic/genetic diversity patterns, and ecological modeling are in agreement with what is expected for P–D model of speciation. While some morphological traits of *P. ludlowii* (the D taxon) can be considered new compared to *P. delavayii* (the P species), such as the number of carpels, others could be the result of the fixation of a given trait among the variability of the P species (e.g., pure yellow corollas). The lack of stolons in *P. ludlowii* can also be viewed as the fixation of a very rare trait within *P. delavayi* (as the vast majority of populations shows a vigorous vegetative propagation; Hong, 2010). Regarding genetic diversity, *P. ludlowii* shows only a subset of the variability of the putative progenitor (values of P_{99}, *A*, *AR* and H_e are much higher for *P. delavayi* compared to *P. ludlowii*; Table 2) with few unique alleles (three exclusive alleles for *P. ludlowii* compared to 89 for *P. delavayi*).

Niche similarity tests are suggestive that there is at least some degree of niche divergence

of *P. ludlowii* with respect to *P. delavayi*. According to the background tests, the niche model of *P. delavayi* can predict the niche of *P. ludlowii* (i.e., niche conservatism), but the model of *P. ludlowii* is not able to predict that of *P. delavayi* (i.e., niche differentiation, Fig. S6), which can also be visualized in the habitat suitability maps (Fig. 7). Such asymmetrical niche differentiation may be due to limited availability of the preferred environmental conditions within the range of the species showing greater differentiation than expected (e.g., Culumber et al., 2012) or to some degree of habitat selection or specialization within a range of environmental conditions (e.g., Sackett et al., 2014). Compared to *P. delavayi*, *P. ludlowii* has a much narrower niche (its niche breadth is below one-fifth that of *P. delavayi*), whereas its current populations tend to occur at higher elevations (altitude = 3588 ± 429 m vs. 3010 ± 637 m), at colder (mean annual temperature = 6.9 ± 2.4 ºC vs. 9.3 ± 3.8; mean temperature of coldest quarter = −5.8 ± 2.5 ºC vs. 2.5 ± 4.2 ºC) and at clearly much drier (annual precipitation = 603 ± 100 mm vs. 882 ± 154 mm) sites. This putative specialization of *P. ludlowii* toward the harsher upland Tibetan conditions is fully compatible with the scenario of a P–D model of speciation.

Instead of remaining unchanged, as stated by the classical definition of a P–D species pair, *P. delavayi* itself seems to be in process of differentiation, which is mainly (but not exclusively) allopatric. As noted in the Introduction, none of the multiple variants of *P. delavayi* (often described as subspecies or varieties, or even as 'species') has merited taxonomic recognition (Hong et al., 1998, Hong, 2010). We believe that the variations of the morphological characters that were used to define these entities might represent, however, the fixation of a given character (within the polymorphism of the species) at the local level [e.g., yellow petals in Eryuan of NW Yunnan (*P. lutea*), or withish petals around Weixi of NW Yunnan (*P. weisiensis*)]. Genetic data, rather than morphology, unambiguously indicate the onset of an ongoing speciation process within *P. delavayi*: indeed, the Tibetan populations of *P. delavayi* as a whole are in an advanced process of divergence, as shown in all our genetic analyses (Figs. 3, 4, 5 and S1), and may merit recognition as a distinct evolutionary lineage. In addition, the Sichuan and Yunnan populations are also showing clear signals of genetic divergence among them; notably, genetic structure Bayesian approaches indicate that, as a general norm, each population has its own cluster. F_{ST} values among populations are very high for nuclear (around 50%; Tables 3 and 4) markers and extremely so for chloroplast markers (98%; Table 3). Although divergence based on plastid DNA was only slightly lower, F_{ST} values based on nSSR were much lower (0.302 *vs.* 0. 510) for another tree peony, *Paeonia rockii* (Yuan et al., 2011, 2012); this is a very pertinent comparison given that the same set of nSSR were used, although it should be taken into account that *P. rockii* reproduces exclusively by sexual means (Chen et al., 1997). A series of life-history traits, in addition to topographical isolation (the Hengduan Mountains have an extremely complex topography, with elevation gradients of up to 5000 m), might act as stimuli for the incipient allopatric differentiation: (1) a general poor performance of sexual reproduction observed in the field (despite that *P. delavayi* may be outcrossing; Li et al., 2014), (2) lack of adaptation of seeds to long-distance dispersal, and (3) the (likely) preponderance of clonal propagation (Hong et al., 1998; Hong, 2010; Li et al., 2012). The isolation-by-distance found among *P. delavayi* populations is also supporting this pattern.

4.2. Genetic diversity and phylogeography: the role of Hengduan Mountains as a refugium for subsect. *Delavayanae*

529 The high richness of plant species in China, especially the overrepresentation of relict
530 lineages, has been ascribed to the existence of large refugial areas (partly due to the lack of
531 Pleistocene extensive glaciations; López-Pujol et al., 2011; Huang et al., 2015). Although large
532 glaciers existed in the QTP, these never formed a unified ice sheet such as Fennoscandia and
533 Laurentide ones (Li et al., 1991; Shi, 2002; Owen et al., 2008; Kirchner et al., 2011). The low-
534 altitude parts of the Hengduan Mountains mostly remained ice-free, especially at its
535 southernmost section (Li et al., 1991; Shi, 2002). Indeed, the Hengduan Mountains are regarded
536 as a Pleistocene glacial refugium (Zhang et al., 2009b; López-Pujol et al., 2011; Qiu et al., 2011;
537 Liu et al., 2012; Tang, 2015); even very relic elements, such as *Cunninghamia lanceolata* Lamb,
538 *Davidia involucrata* Baill. or *Taiwania cryptomerioides* Hayata, found a refugium in the
539 southern Hengduan Mountains, where temperature and precipitation kept relatively high even
540 during the LGM (e.g., Jiang et al., 2011; Lu et al., 2013; Liu and Jiang, 2016; Tian and Jiang,
541 2016). Despite that levels of genetic diversity of *P. delavayi* as a whole are lower than those of
542 *Paeonia rockii* (Yuan et al., 2012), it should be taken into account that the latter occurs in an
543 area (Qinling and central China ranges) that was never glaciated and was home of some of the
544 most important glacial refugia of China (e.g., López-Pujol et al., 2011; Huang et al., 2015).
545 Indeed, if we consider only those populations located in areas that were ice-free or almost ice-
546 free (those at latitudes below 28ºN), then the levels of genetic diversity of *P. delavayi*
547 populations (H_e = 0.448) are closer to those of *Paeonia rockii* (H_e = 0.498; Yuan et al., 2012)
548 and even higher to those expected for endemic species (H_e = 0.420; Nybom, 2004).
549 Judging from the values of polymorphism included in Table 2, it seems that the extent of
550 glaciers and ice caps at the LGM within the Hengduan Mountains would have played a major
551 role in the genetic variability harbored by the populations of *P. delavayi*, as found for other
552 regional endemisms [e.g., *Sinopodophyllum hexandrum* (Royle) T.S. Ying; Li et al., 2011]. We
553 believe that this is a reliable assumption given that microsatellites, mainly due to their high
554 mutation rates and high incidence of homoplasy, are generally only suitable to reveal events on
555 timescales of just several thousands of years (Jarne and Lagoda, 1996). Almost all populations
556 located in the south section of Hengduan Mountains (DY-XIG, DY-DAL, DY-WEI2, and DY-
557 LIJ)—that was relatively ice-free at the LGM (Fig. 8), would have been refugial for *P. delavayi*,
558 because they show a large number of alleles (including private ones) and show the highest H_e
559 values (Table 2); in fact, mean H_e values of these four populations plus DY-WEI1 (H_e = 0.460,
560 SD = 0.067) are much larger as a whole than those of the four populations (DY-DEQ, DS-XIA,
561 DS-LIT, and DS-MUL) located in the northern section of the Hengduan mountains, much more
562 affected by glaciations (H_e = 0.314, SD = 0.071). The Lijiang-Xianggelila region probably
563 harbored the most important refuges for the taxon, as these are the only two populations (DY-
564 LIJ and DY-XIG) that show partial membership to multiple clusters at K = 13 (Fig. 5).
565 Xianggelila, in addition, is the population harboring the highest number of alleles, while almost
566 all described petal colours have been observed there (which could be the result of secondary
567 contact of yellow and deep-pink flowered morphotypes; Hong et al., 1998; Hong, 2010; Zhang
568 et al., 2011). Pollen records indicate the presence of broad-leaved forests [*Quercus* L., *Betula*
569 L. and *Castanopsis* (D. Don) Spach; Yao et al., 2015] in the area, suggesting certain level of
570 climatic stability. Under such scenario, populations would have maintained relatively large
571 sizes while keeping certain levels of gene flow.
572 The northern populations (i.e., DY-DEQ, DS-XIA, DS-LIT, and DS-MUL) of *P. delavayi*

probably escaped the coldest periods of the Pleistocene by means of downward migrations to the adjacent valleys. All these populations, although showing low levels of heterozygosity, harbor exclusive allele variants (Table 2), suggesting *in situ* persistence. Glaciers here were more extensive (Fu et al., 2013) and populations, perhaps with the single exception of DS-XIA (which has the highest heterozygosity among this group; Table 2), would have directly been affected by LGM ice caps (as populations were located on the surroundings of these; Fig. 8). Moreover, the northern part of the Hengduan Mountains was colder and drier than the southern one, even showing more differences than at present (Jiang et al., 2011; Tian and Jiang, 2016), which would have favoured the persistence of the taxon in microrefugia instead of macrorefugia (Rull, 2009). On the contrary, the nSSR data suggest that the Tibetan populations of *P. delavayi* might be the result of recent recolonizations (perhaps after the LGM): both their levels of heterozygosity and number of alleles are the lowest within the taxon, and have no exclusive alleles (with the exception of DT-BOM1; Table 2). The mountain range that dominated this area, Nyainqêntanglha, was extensively glaciated at the LGM, and the three populations (DT-BOM1, DT-BOM2, and DT-NYI) are located in an area that was supposedly covered by ice caps at the LGM (Li et al., 1991; Fig. 8).

ENM results are equivocal, given that the three models (CCSM, MIROC, and MPI) indicate a very different scenario for *P. delavayi* at the LGM (Figs. 7 and S5). The MIROC model seems to be unrealistic, as most of the reconstructed suitable areas occur in regions that were heavily glaciated (Li et al., 1991; Shi, 2002; Fig. 8) and the 'lost' area compared to the present corresponds to the more polymorphic populations (Fig. S5). Both the CCSM and MPI models (especially the latter) basically agree with the continuous presence of the taxon in southern macrorefugia (Figs. 7 and S5), a scenario compatible with the mismatch analysis (Fig. S4). The ENM also indicates a slight decrease in the mean altitude of the suitable habitats for *P. delavayi* at the LGM compared to the present (of about 300 m; Table S7). It is agreed that mountain species would have tracked the Pleistocene climatic oscillations by means of altitudinal changes; admixture as consequence of downward migrations in the colder periods would have blurred genetic footprints of allopatric divergence, as it is often reported in plants inhabiting the mountains of the Mediterranean Basin (Nieto-Feliner, 2014; Jiménez-Mejías et al., 2015) and the Korean Peninsula (Chung et al., 2017). For *P. delavayi*, the large altitudinal gradients generally prevented populations from secondary contacts among closely-located populations (with some exceptions, e.g., Xianggelila) and, therefore, did not compensate the strong geographical isolation that is found at present (there is almost a total absence of ongoing recent gene flow; Table S6). Low seed production and seedling establishment, aggravated by the lack of adaptation to long-distance dispersal of *P. delavayi* seeds (Hong, 2010) might have contributed to avoid wider altitudinal displacements.

The haplotype distribution within and among *P. delavayi* populations also indicates that this taxon survived in multiple refugia in the Hengduan Mountains, in agreement with microsatellites. Most populations are fixed for a single haplotype and, with the exception of H1, no haplotypes are present in more than one population (Fig. 1A). Judging from the high number of missing haplotypes, local extinction would have also been common, as expected for a region that was partially covered by ice caps. However, plastid DNA may also reflect older events; extinction of haplotypes and generation of new ones would have also been the result of mountain building episodes, some of which took place until very recent phases of the

Pleistocene. Although there is still much controversy regarding the tempo and pace of the major uplift events of the QTP, there is relative consensus on the fact that Hengduan Mountains are of very recent origin, probably with abrupt upliftings during the Pliocene (Favre et al., 2015) and probably extending into the Pleistocene (e.g., Li and Fang, 1999). However, as no mutation rates are available for plastid DNA of *Paeonia*, we are not able to distinguish whether the phylogeographic patterns are mainly attributable to geologic or to climatic events. The oldest divergence event detected in our cpDNA network (that between haplotypes H1 and H7; Fig. 1B) may even pre-date the Hengduan Mountains uplift.

In agreement with microsatellites, the haplotype architecture of *P. delavayi* is also suggesting that the three Tibetan populations (DT-BOM1, DT-BOM2, and DT-NYI) could have been the result of migration from warmer places (most probably at lower elevations in the Hengduan Mountains), after the retreat of the glaciers that almost completely covered the eastern section of Nyainqêntanglha range (where the three populations are located; see Fig. 8). Regarding *P. ludlowii*, all the studied populations are fixed for a single haplotype (H2) that, according to the haplotype network, it is a derived one. However, the fact that the H2 haplotype appears as basal to haplotypes H4 and H5 in the Bayesian tree (Fig. 2) and the many mutational steps (9–11) that separates H2 from its closest haplotypes both indicate a long isolation of these populations, probably mainly driven by genetic drift. Such isolation is also indicated by the Barrier analyses (Fig. 6), and would have been accompanied by a process of ecological specialization that it is almost complete. The fixation of some morphological characters (e.g., low number of carpels and lack of stolons) should be viewed in the context of this speciation process (Liu et al., 2014). The extremely low levels of hetezygosity and allelic richness as revealed by nSSR are expected for a scenario of long-term persistence [in or around (micro)refugia] within a heavily glaciated area (Fig. 8) under extreme cold and dry conditions (e.g., Tian and Jiang, 2016), in which populations were probably small and isolated. Therefore, we can propose a dual model for subsect. *Delavayanae*, in which the two main hypotheses of Quaternary history of QTP plant species are not mutually exclusive: (i) *in situ* persistence in local refugia in the QTP and (ii) *tabula rasa* (retreat to SE refugia in glacial periods followed by recolonization in postglacial ones) (Qiu et al., 2011; Liu et al., 2014). Such a double scenario has also been reported in other regional endemics including *Sinopodophyllum hexandrum* (Royle) T.S. Ying (Li et al., 2011), *Lepisorus clathratus* Ching (Wang et al., 2011), or *Anisodus tanguticus* Pascher (Wan et al., 2016).

4.3. Conclusions: evolutionary and conservation remarks

The HHM region, but especially the Hengduan Mountains, is probably the largest 'evolutionary front' of the world's North Temperate Zone (López-Pujol et al., 2011). Some of the most amazing plant radiations are taking place there, with lineages in which dozens to hundreds of new species have arisen in the last million years (Wen et al., 2014; Hugues and Atchison, 2015). For some extreme cases of 'rapid' radiations, each species can be limited to a single mountain (Zhang et al., 2009b). In contrast to some of these spectacular examples, such as *Pedicularis* or *Saussurea*, our case study (subsect. *Delavayanae*) could be regarded as a sort of a 'slow', gradual radiation, and this 'slowness' in its diversification could be partly due to the demographic dynamics of the species; the population viability of both *P. delavayi* and *P. ludlowii* seems to mainly rely on longevity (individuals of both taxonomic entities usually reach

15–20 years; Yang et al., 2007; Li et al., 2012) which makes recruitment (which is rare in the field; He, 2008; Hong, 2010) relatively unnecessary, especially for the case of *P. delavayi*. Our results indicate that at present at least three entities are clearly recognizable on the genetic grounds (what is known as *P. ludlowii*, the Sichuan/Yunnan populations of *P. delavayii*, and the Tibetan populations of *P. delavayi*), with the two latter not morphologically recognizable yet. Carrying out additional studies may help to understand the ongoing speciation process, and these may include (1) examining the stability of the diagnostic morphological traits (through common-garden experiments); and (2) seeing, through comparative pollination studies, whether pollinators have effectively influenced the fixation of floral and reproductive traits and thus, the extent (if any) of pollinator-driven ecological speciation. Indeed, the preliminary results of Shuai and Zang (2016) suggest that *P. ludlowii* has a wider spectrum of pollinators—with higher frequencies of visits—compared to *P. delavayi*, and that insects show some degree of phenotypic selection regarding several floral traits (e.g., petal length and petal width) which is also variable between the two taxa. Although further studies are needed, such results might indicate that pollinators play some role in the process of ecological differentiation of *P. ludlowii*.

The rarity of *P. ludlowii* and high evolutionary potential of *P. delavayi* imply high priority of *in situ* conservation of both taxa. Considering the high genetic differentiation among populations of *P. delavayi* and variable morphology, and given that this taxon is under active speciation, as many populations as possible should be conserved. Its extensive harvest due to the medicinal properties (Hong, 2010; Yang et al., 2014), as well as its habitat fragmentation (mainly as consequence of tourism growth, road construction, and economic development in general; e.g., Gu et al., 2013; Ye et al., 2015), if not banned or stopped, might contribute to further increases in genetic differentiation, as it has been reported in the literature (e.g., Cruse-Sanders and Hamrick, 2004; Chung et al., 2014). As for further conservation efforts for *P. delavayi*, these should be directed towards the most polymorphic populations (and putatively contact zones), which, based on our results, are located in NW Yunnan: the axis Lijiang-Xianggelila, Weixi, and Dali.

Acknowledgements

We thank Yi Wang and Jianxiu Wang for their field and technical assistance and helpful discussion. Special thanks goes to Sonia Herrando-Moraira for her help in drawing Fig. 8 and for her insightful commentaries. This study was supported by the National Natural Science Foundation of China (NSFC 30121003) and the Ministry of Science and Technology of China (2012BAC01B05).

Appendix A. Suplementary material

Supplementary data associated with this article can be found, in the online version at http://xxxxxxxxxxxxxxxxxxxx.

References

Barthlott, W., Mutke, J., Rafiqpoor, D., Kier, G., Kreft, H., 2005. Global centers of vascular

plant diversity. Nova Acta Leopold. 92, 61–83.
Belkhir, K., Borsa, P., Chikhi, L., Raufaste, N., Bonhomme, F., 1996–2004. GENETIX 4.05, logiciel sous Windows^{TM} pour la génétique des populations. Laboratoire Génome, Populations, Interactions, CNRS UMR 5000, Université de Montpellier II, Montpellier.
Chapuis, M.-P., Estoup, A., 2007. Microsatellite null alleles and estimation of population differentiation. Mol. Biol. Evol. 24, 621–631.
Chapuis, M.-P., Lecoq, M., Michalakis, Y., Loiseau, A., Sword, G.A., Piry, S., Estoup, A., 2008. Do outbreaks affect genetic population structure? A worldwide survey in *Locusta migratoria*, a pest plagued by microsatellite null alleles. Mol. Ecol. 17, 3640–3653.
Chen, F., Li, J., Chen, D., 1997. The natural propagation characteristics of wild tree peony species in China. Acta Hortic. Sin. 24, 180–184.
Chung, M.Y., López-Pujol, J. Chung, M.G., 2017. The role of the Baekdudaegan (Korean Peninsula) as a major glacial refugium for plant species: A priority for conservation. Biol. Conserv. 206, 236–248.
Chung, M.Y., Nason, J.D., López-Pujol, J., Yamashiro, T., Yang, B.-Y., Luo, Y.-B., Chung, M.G., 2014. Genetic consequences of fragmentation on populations of the terrestrial orchid *Cymbidium goeringii*. Biol. Conserv. 170, 222–231.
Clement, M., Posada, D., Crandall, K.A., 2000. TCS: a computer program to estimate gene genealogies. Mol. Ecol. 9, 1657–1660.
Cornuet, J.M., Luikart, G., 1996. Description and power analysis of two tests for detecting recent population bottlenecks from allele frequency data. Genetics 144, 2001–2014.
Crawford, D.J., 2010. Progenitor-derivative species pairs and plant speciation. Taxon 59, 1413–1423.
Cruse-Sanders, J.M., Hamrick, J.L., 2004. Genetic diversity in harvested and protected populations of wild American ginseng, *Panax quinquefolius* L. (Araliaceae). Am. J. Bot. 91, 540–548.
Culumber, Z.W., Shepard, D.B., Coleman, S.W., Rosenthal, G.G., Tobler, M., 2012. Physiological adaptation along environmental gradients and replicated hybrid zone structure in swordtails (Teleostei: *Xiphophorus*). J. Evol. Biol. 25, 1800–1814.
Dakin, E.E., Avise, J.C., 2004. Microsatellite null alleles in parentage analysis. Heredity 93, 504–509.
Dempster, A., Laird, N., Rubin, D., 1977. Maximum likelihood from incomplete data via the EM algorithm. J. R. Stat. Soc. Series B Stat. Methodol. 39, 1–38.
Dieringer, D., Schlötterer, C., 2003. Microsatellite analyser (MSA): a platform independent analysis tool for large microsatellie data sets. Mol. Ecol. Notes 3, 167–169.
Earl, D.A., vonHoldt, B.M., 2012. STRUCTURE HARVESTER: a website and program for visualizing STRUCTURE output and implementing the Evanno method Conserv. Genet. Resour. 4, 359–361.
Evanno, G., Regnaut, S., Goudet, J., 2005. Detecting the number of clusters of individuals using the software STRUCTURE: a simulation study. Mol. Ecol. 14, 2611–2620.
Excoffier, L., Lischer, H.E.L., 2010. Arlequin suite ver 3.5: A new series of programs to perform population genetics analyses under Linux and Windows. Mol. Ecol. Resour. 10, 564–567.
Favre, A., Päckert, M., Pauls, S.U., Jähnig, S.C., Uhl, D., Michalak, I., Muellner-Riehl, A.N., 2015. The role of the uplift of the Qinghai-Tibetan Plateau for the evolution of Tibetan

biotas. Biol. Rev. 90, 236–253.
Fu, P., Harbor, J.M., Stroeven, A.P., Hättestrand, C., Heyman, J., Zhou, L., 2013. Glacial geomorphology and paleoglaciation patterns in Shaluli Shan, the southeastern Tibetan Plateau — Evidence for polythermal ice cap glaciation. Geomorphology 182, 66–78.
Fu, Y.X., 1997. Statistical tests of neutrality of mutations against population growth, hitchhiking and background selection. Genetics 147, 915–925.
Fu, Y.X., Li, W.H., 1993. Statistical tests of neutrality of mutations. Genetics 133, 693–709.
Gottlieb, L.D., 2003. Rethinking classic examples of recent speciation in plants. New Phytol. 161, 71–82.
Goudet, J., 1995. FSTAT (Version 1.2): A computer program to calculate F-statistics. J. Hered. 86, 485–486.
Gu, Y., Du, J., Tang, Y., Qiao, X., Bossard, C., Deng, G., 2013. Challenges for sustainable tourism at the Jiuzhaigou World Natural Heritage site in western China. Nat. Resour. Forum 37, 103–112.
Harpending, H.C., 1994. Signature of ancient population growth in a low-resolution mitochondrial DNA mismatch distribution. Hum. Biol. 66, 591–600.
He, Z., 2008. Seed dormancy and germination characteristics of *Paeonia ludlowii*, an endangered plant endemic to China. PhD Thesis, Institute of Botany, Chinese Academy of Sciences, Beijing (in Chinese).
He, S.-A., Xing, F.-W., 2015. Ornamental plants. In: Hong, D.-Y., Blackmore, S. (Eds.), Plants of China, a companion to the Flora of China. Science Press, Beijing, pp. 342–356.
Hijmans, R.J., Camerson, S.E., Parra, J.L., Jone, P.G., Javis, A., 2005. Very high solution interpolated climate surfaces for global land areas. Int. J. Climatol. 25, 1965–1978.
Hong, D.-Y., 1997. *Paeonia* (Paeoniaceae) in Xizang (Tibet). Novon 7, 156–161.
Hong, D.-Y., 2010. Peonies of the world. Taxonomy and phytogeography. Royal Botanical Gardens Kew–Missouri Botanical Garden, London–St. Louis.
Hong, D.-Y., Pan, K.-Y., Hong, Y., 1998. Taxonomy of the *Paeonia delavayi* complex (Paeoniaceae). Ann. Mo. Bot. Gard. 85, 554–564.
Huang, P., Schaal, B.A., 2012. Association between the geographic distribution during the last glacial maximum of Asian wild rice, *Oryza rufipogon* (Poaceae), and its current genetic variation. Am. J. Bot. 99, 1866–1874.
Huang, Y., Jacques, F.M.B., Su, T., Ferguson, D.K., Tang, H., Chen, W., Zhou, Z., 2015. Distribution of Cenozoic plant relicts in China explained by drought in dry season. Sci. Rep. 5, 14212.
Hugues, C.E., Atchison, G.W., 2015. The ubiquity of alpine plant radiations: from the Andes to the Hengduan Mountains. New Phytol. 207, 275–282.
Hurlbert, S.H., 1971. The nonconcept of species diversity: a critique and alternative parameters. Ecology 52, 577–586.
Jakobsson, M., Rosenberg, N.A., 2007. CLUMPP: a cluster matching and permutation program for dealing with label switching and multimodality in analysis of population structure. Bioinformatics 23, 1801–1806.
Janes J.K., Miller J.M., Dupuis J.R., Malenfant R.M., Gorrell J.C., Cullingham C.I., Andrew R.L., 2017. The $K = 2$ conundrum. Mol. Ecol. 26, 3594–3602.
Jarne, P. Lagoda, P., 1996. Microsatellites, from molecules to populations and back. Trends

Ecol. Evol. 11, 424–429.
Jensen, J.L., Bohonak, A.J., Kelley, S.T., 2005. Isolation by distance, web service. BMC Genet. 6, 13.
Jiang, D., Lang, X., Tian, Z., Guo, D., 2011. Last glacial maximum climate over China from PMIP simulations. Palaeogeogr. Palaeoclimatol. Palaeoecol. 309, 347–357.
Jiménez-Mejías, P., Fernández-Mazuecos, M., Amat, M.E., Vargas, P., 2015. Narrow endemics in European mountains: high genetic diversity within the monospecific genus *Pseudomisopates* (Plantaginaceae) despite isolation since the late Pleistocene. J. Biogeogr. 42, 1455–1468.
Kirchner, N., Greve, R., Stroeven, A.P., Heyman, J., 2011. Paleoglaciological reconstructions for the Tibetan Plateau during the last glacial cycle: evaluating numerical ice sheet simulations driven by GCM-ensembles. Quat. Sci. Rev. 30, 248–267.
Langella, O., 1999. Populations, v.1.2.28, available from <http://bioinformatics.org/~tryphon/populations>.
Levins, R., 1968. Evolution in changing environments. Princeton University Press, Princeton.
Li, B., Li, J., Cui, Z., Zheng, B., Zhang, Q., Wang, F., Zhou, S., Shi, Z., Jiao, K., Kang, J., 1991. Quaternary glacial distribution map of Qinghai-Xizang (Tibet) Plateau 1:3,000 000. Science Press, Beijing.
Li, J., Fang, X., 1999. Uplift of the Tibetan Plateau and environmental changes. Chin. Sci. Bull. 44, 2117–2124.
Li, J., Wang, S., Jing, Y., Wang, L., Zhou, S., 2013. A modified CTAB protocol for plant DNA extraction. Chin. Bull. Bot. 48, 72–78.
Li, K., Zheng, B., Wang, Y., Zhou, L., 2014. Breeding system and pollination biology of *Paeonia delavayi* (Paeoniaceae), an endangered plant in the southwest of China. Pak. J. Bot. 46, 1631–1642.
Li, K., Zheng, B.-Q., Wang, Y., Bu, W.-S., 2012. Numeric dynamics of natural populations of *Paeonia delavayi* (Paeoniaceae). Chin. J. Plant Ecol. 36, 522–529 (in Chinese).
Li, Y., Zhai, S.N., Qiu, Y.X., Guo, Y.P., Ge, X.J., Comes, H.P., 2011. Glacial survival east and west of the 'Mekong-Salween Divide' in the Himalaya-Hengduan Mountains region as revealed by AFLPs and cpDNA sequence variation in *Sinopodophyllum hexandrum* (Berberidaceae). Mol. Phylogenet. Evol. 59, 412–424.
Librado, P., Rozas, J., 2009. DnaSP v5: a software for comprehensive analysis of DNA polymorphism data. Bioinformatics 25, 1451–1452.
Liu, J., Möller, M., Provan, J., Gao, L.-M., Poudel, R.C., Li, D.-Z., 2013. Geological and ecological factors drive cryptic speciation of yews in a biodiverity hotspot. New Phytol. 199, 1093–1108.
Liu, J.-Q., Duan, Y.-W., Hao, G., Ge, X.-J., Sun, H., 2014. Evolutionary history and underlying adaptation of alpine plants on the Qinghai-Tibet Plateau. J. Syst. Evol. 52, 241–249.
Liu, J.-Q., Sun, Y.-S., Ge, X.-J., Gao, L.-M., Qiu, Y.-X., 2012. Phylogeographic studies of plants in China: advances in the past and directions in the future. J. Syst. Evol. 50, 267–275.
Liu, Y., Jiang, D., 2016. Last glacial maximum permafrost in China from CMIP5 simulations. Palaeogeogr. Palaeoclimatol. Palaeoecol. 447, 12–21.
López-Pujol, J., Zhang, F.-M., Sun, H.-Q., Ying, T.-S., Ge, S., 2011. Centres of plant endemism in China: places for survival or for speciation? J. Biogeogr. 38, 1267–1280.

Lu, H., Yi, S., Liu, Z., Mason, J.A., Jiang, D., Cheng, J., Stevens, T., Xu, Z., Zhang, E., Jin, L., Zhang, Z., Guo, Z., Wang, Y., Otto-Bliesner, B., 2013. Variation of East Asian monsoon precipitation during the past 21 k.y. and potential CO_2 forcing. Geology 41, 1023–1026.

Luikart, G., Cornuet, J.M., 1998. Empirical evaluation of a test for identifying recently bottlenecked populations from allele frequency data. Conserv. Biol. 12, 228–237.

Luo, D., Yue, J-P., Sun, W-G., Xu, B., Li, Z-M., Comes, H.P., Sun, H., 2016. Evolutionary history of the subnival flora of the Himalaya-Hengduan Mountains: first insights from comparative phylogeography of four perennial herbs. J. Biogeogr. 43, 31–43.

Manni, F., Guerard, E., Heyer, E., 2004. Geographic patterns of (genetic, morphologic, linguistic) variation: how barriers can be detected by using Monmonier's algorithm. Hum. Biol. 76, 173–190.

Mantel, N., 1967. The detection of disease clustering and a generalized regression approach. Cancer Res. 27, 209–220.

MEP–CAS (Ministry of Environmental Protection–Chinese Academy of Sciences), 2013. China red list of higher plants. Ministry of Environmental Protection of the People's Republic of China and Chinese Academy of Sciences, Beijing [in Chinese].

Mittermeier, R.A., Turner, W.R., Larsen, F.W., Brooks, T.M., Gascon, C., 2011. Global biodiversity conservation: The critical role of hotspots. In: Zachos, F.E., Habel, J.C. (Eds.), Biodiversity hotspots. Distribution and protection of conservation priority areas. Springer-Verlag, Berlin-Heidelberg, pp. 3–22.

Mulch, A., Camberlain, C.P., 2006. The rise and growth of Tibet. Nature 439, 670–671.

Nei, M., 1972. Genetic distance between populations. Am. Nat. 106, 289–291.

Nei, M., 1978. Estimation of average heterozygosity and genetic distance from a small number of ndividuals. Genetics 89, 583–590.

Nei, M., Tajima, F., Tateno, Y., 1983. Accuracy of estimated phylogenetic trees from molecular data. J. Mol. Evol. 19, 153–170.

Nieto-Feliner, G., 2014. Patterns and processes in plant phylogeography in the Mediterranean Basin. A review. Perspect. Plant Ecol. Evol. Syst. 16, 265–278.

Nybom, H., 2004. Comparison of different nuclear DNA markers for estimating intraspecific genetic diversity in plants. Mol. Ecol. 13, 1143–1155.

Orsini, L., Corander, J., Alasentie, A., Hanski, I., 2008. Genetic spatial structure in a butterfly metapopulation correlates better with past than present demographic structure. Mol. Ecol. 17, 2629–2642.

Owen, L.A., Caffee, M.W., Finkel, R.C., Seong, Y.B., 2008. Quaternary glaciation of the Himalayan-Tibetan orogen. J. Quaternary Sci. 23, 513–531.

Page, R.D.M., 1996. TREEVIEW: an application to display phylogenetic trees on personal computers. Comput. Appl. Biosci. 12, 357–358.

Peakall, R., Smouse, P.E., 2006. GENALEX 6: genetic analysis in Excel. Population genetic software for teaching and research. Mol. Ecol. Notes 6, 288–295.

Pearson, R.G., Raxworthy, C.J., Nakamura, M., Peterson, A.T., 2007. Predicting species distributions from small numbers of occurrence records: a test case using cryptic geckos in Madagascar. J. Biogeogr. 34, 102–117.

Phillips, S.J., Anderson, R.P., Schapire, R.E., 2006. Maximum entropy modeling of species geographic distributions. Ecol. Model. 190, 231–259.

881 Piry, S., Luikart, G., Cornuet, J., 1999. Computer note. BOTTLENECK: a computer program
882 for detecting recent reductions in the effective size using allele frequency data. J. Hered.
883 90, 502–503.
884 Pons, O., Petit, R.J., 1996. Measuring and testing genetic differentiation with ordered versus
885 unordered alleles. Genetics 144, 1237–1245.
886 Posada, D., 2008. jModelTest: Phylogenetic model averaging. Mol. Biol. Evol. 25, 1253–1256.
887 Pritchard, J.K., Stephens, M., Donnelly, P., 2000. Inference of population structure using
888 multilocus genotype data. Genetics 155, 945–959.
889 Pritchard, J.K., Wen, X., Falush, D., 2010. Documentation for Structure software: Version 2.3.:
890 Department of Human Genetics, University of Chicago. Chicago.
891 https://web.stanford.edu/group/pritchardlab/structure_software/release_versions/v2.3.4/st
892 ructure_doc.pdf
893 Qiu, Y.-X., Fu, C.-X., Comes H.P., 2011. Plant molecular phylogeography in China and adjacent
894 regions: tracing the genetic imprints of Quaternary climate and environmental change in
895 the world's most diverse temperate flora. Mol. Phylogenet. Evol. 59, 225–244.
896 Ramos-Onsins, R., Rozas, R., 2002. Statistical properties of new neutrality tests against
897 population growth. Mol. Biol. Evol. 19, 2092–2100.
898 Rice, W.R., 1989. Analyzing tables of statistics tests. Evolution 43, 223–225.
899 Rogers, A.R., Harpending, H., 1992. Population growth makes waves in the distribution of
900 pairwise genetic differences. Mol. Biol. Evol. 9, 552–569.
901 Rogers, J.S., 1972. Measures of genetic similarity and genetic distance. Studies in genetics VII.
902 Univ. Texas Publ. 7213, 145–153.
903 Ronquist, F., Huelsenbeck, J.P., 2003. MrBayes 3: Bayesian phylogenetic inference under
904 mixed models. Bioinformatics 19, 1572–1574.
905 Rosenberg, N.A., 2004. DISTRUCT: A program for the graphical display of population
906 structure. Mol. Ecol. Notes 4, 137–138.
907 Rousset, F., 1997. Genetic differentiation and estimation of gene flow from F-statistics under
908 isolation by distance. Genetics 145, 1219–1228.
909 Rull, V., 2009. Microrefugia. J. Biogeogr. 36, 481–484.
910 Sackett, L.C., Seglund, A., Guralnick, R.P., Mazzella, M.N., Wagner, D.M., Busch, J.D., Martin,
911 A.P., 2014. Evidence for two subspecies of Gunnison's prairie dogs (*Cynomys gunnisoni*),
912 and the general importance of the subspecies concept. Biol. Conserv. 174, 1–11.
913 Schwery, O., Onstein, R.E., Bouchenak-Khelladi, Y., Xing, Y., Carter, R.J., Linder, H.P., 2015.
914 As old as the mountains: the radiations of the Ericaceae. New Phytol. 207, 355–367.
915 Shi, Y., 2002. Characteristics of late Quaternary monsoonal glaciation on the Tibetan Plateau
916 and in East Asia. Quat. Int. 97–98, 79–91.
917 Shuai, Y.-T., Zang, J.-C., 2016. *Paeonia ludlowii* and *Paeonia delavayi* flower characteristics
918 and change of flower-visiting insects and phenotypic selection. Southwest China J. Agric.
919 Sci. 29, 2714–2719 (in Chinese).
920 Swofford, D.L., 2002. PAUP*: Phylogenetic Analysis Using Parsimony (*and other methods),
921 ver. 4.0b410. Sinauer Associates, Sunderland.
922 Tajima, F., 1989. Statistical method for testing the neutral mutation hypothesis by DNA
923 polymorphism. Genetics 123, 585–595.
924 Tang, C.Q., 2015. The subtropical vegetation of Southwestern China. Plant distribution,

diversity and ecology. Springer, Dordrecht.
Tian, Z., Jiang, D., 2016. Revisiting last glacial maximum climate over China and East Asian monsoon using PMIP3 simulations. Palaeogeogr. Palaeoclimatol. Palaeoecol. 453, 115–126.
Wan, D.-S., Feng, J.-J., Jiang, D.-C., Mao, K.-S., Duan, Y.-W., Miehe, G., Opgenoorth, L., 2016. The Quaternary evolutionary history, potential distribution dynamics, and conservation implications for a Qinghai–Tibet Plateau endemic herbaceous perennial, *Anisodus tanguticus* (Solanaceae). Ecol. Evol. 6, 1977–1995.
Wang, H., Qiong, L., Sun, K., Lu, F., Wang, Y., Song, Z., Wu, Q., Chen, J., Zhang, W., 2010. Phylogeographic structure of *Hippophae tibetana* (Elaeagnaceae) highlights the highest microrefugia and the rapid uplift of the Qinghai-Tibetan Plateau. Mol. Ecol. 19, 2964–2979.
Wang, J.X., Xia, T., Zhang, J.M., Zhou, S.L., 2009. Isolation and characterization of fourteen microsatellites from a tree peony (*Paeonia suffruticosa*). Conserv. Genet. 10, 1029–1031.
Wang, L., Wu, Z.-Q., Bystriakova, N., Ansell, S.W., Xiang, Q.-P., Heinrichs, J., Schneider, H., Zhang, X.-C., 2011. Phylogeography of the Sino-Himalayan fern *Lepisorus clathratus* on 'The Roof of the World'. PLoS ONE 6, e25896.
Warren, D.L., Glor, R.E., Turelli, M., 2010. ENMTools: a toolbox for comparative studies of environmental niche models. Ecography 33, 607–611.
Weir, B.S., Cockerham, C.C., 1984. Estimating F-statistics for the analysis of population structure. Evolution 38, 1358–1370.
Wen, J., Zhang, J.-Q., Nie, Z.-L., Zhong, Y., Sun, H., 2014. Evolutionary diversifications of plants on the Qinghai-Tibetan Plateau. Front. Genet. 5, 4.
Wilson, G.A., Rannala, B., 2003. Bayesian inference of recent migration rates using multilocus genotypes. Genetics 163, 1177–1191.
Wright, S., 1965. The interpretation of genetic population structure by F-statistics with special regard to systems of mating. Evolution 19, 395–420.
Xing, Y., Ree, R.H., 2017. Uplift-driven diversification in the Hengduan Mountains, a temperate biodiversity hotspot. Proc. Natl. Acad. Sci. U.S.A. 114, E3444–E3451.
Yang, F.-S., Qin, A.-L., Li, Y.-F., Wang, X.-Q., 2012. Great genetic differentiation among populations of *Meconopsis integrifolia* and its implication for plant speciation in the Qinghai-Tibetan Plateau. PLoS ONE 7, e37196.
Yang, L., Ahmed, S., Stepp, J.R., Mi, K., Zhao, Y., Ma, J., Liang, C., Pei, S., Huai, H., Xu, G., Hamilton, A.C., Yang, Z.-W., Xue, D., 2014. Comparative homegarden medical ethnobotany of Naxi healers and farmers in Northwestern Yunnan, China. J. Ethnobiol. Ethnomed. 10, 6.
Yang, X.-L., Wang, Q.-J., Lan, X.-Z., Li, C.Y., 2007. Numeric dynamics of the endangered plant population of *Paeonia ludlowii*. Acta Ecol. Sin. 27, 1242–1247 (in Chinese).
Yao, Y.F., Song, X.Y., Wortley, A.H., Blackmore, S., Li, C.S., 2015. A 22 570-year record of vegetational and climatic change from Wenhai Lake in the Hengduan Mountains biodiversity hotspot, Yunnan, Southwest China. Biogeosciences 12, 1525–1535.
Ye, X., Liu, G., Li, Z., Wang, H., Zeng, Y., 2015. Assessing local and surrounding threats to the protected area network in a biodiversity hotspot: the Hengduan Mountains of Southwest China. PLoS ONE 10, e013853.
Yuan, J.-H., Cheng, F.-Y., Zhou, S.-L., 2011. The phylogeographic structure and conservation

genetics of the endangered tree peony, *Paeonia rockii* (Paeoniaceae), inferred from chloroplast gene sequences. Conserv. Genet. 12,1539–1549.

Yuan, J.-H., Cheng, F.-Y., Zhou, S.-L., 2012. Genetic structure of the tree peony (*Paeonia rockii*) and the Qinling Mountains as a geographic barrier driving the fragmentation of a large population. PLoS ONE 7, e34955.

Zhang, D.-C., Zhang, Y.-H., Boufford, D.E., Sun, H., 2009b. Elevational patterns of species richness and endemism for some important taxa in the Hengduan Mountains, southwestern China. Biodivers. Conserv. 18, 699–716.

Zhang, J., Liu, J., Sun, H., Yu, J., Wang, J., Zhou, S., 2011. Nuclear and chloroplast SSR markers in *Paeonia delavayi* (Paeoniaceae) and cross-species amplification in *P. ludlowii*. Am. J. Bot. 98, e346–e348.

Zhang, J., Wang J, Xia T, Zhou, S. 2009a. DNA barcoding: species delimitation in tree peonies. Sci. China C Life Sci. 52, 568–578.

Zhang, Q., Feild, T.S., Antonelli, A., 2015. Assessing the impact of phylogenetic incongruence on taxonomy, floral evolution, biogeographical history, and phylogenetic diversity. Am. J. Bot. 102, 566–580.

Zhou, S.-L., Zou, X.-H., Zhou, Z.-Q., Liu, J., Xu, C., Yu, J., Wang, Q., Zhang, D.-M., Wang, X.-Q., Ge, S., Sang, T., Pan, K.-Y., Hong, D.-Y., 2014. Multiple species of wild tree paeonies gave rise to the ‘king of flowers’, *Paeonia subffruticosa* Andrews. Proc. R. Soc. Lond. B 281, 20141687.

LEGEND OF FIGURES

Fig. 1. (A) Map showing the location of the studied populations of *Paeonia delavayi* and *P. ludlowii* (population codes are given in Table 1) and the distribution of plastid DNA haplotypes. Pie sizes are proportional to the haplotype frequency. (B) Haplotype network constructed by TCS v.1.2.1. The small open circles represent missing haplotypes. The size of coloured circles is approximately proportional to the observed frequency of haplotypes. * = outgroup position.

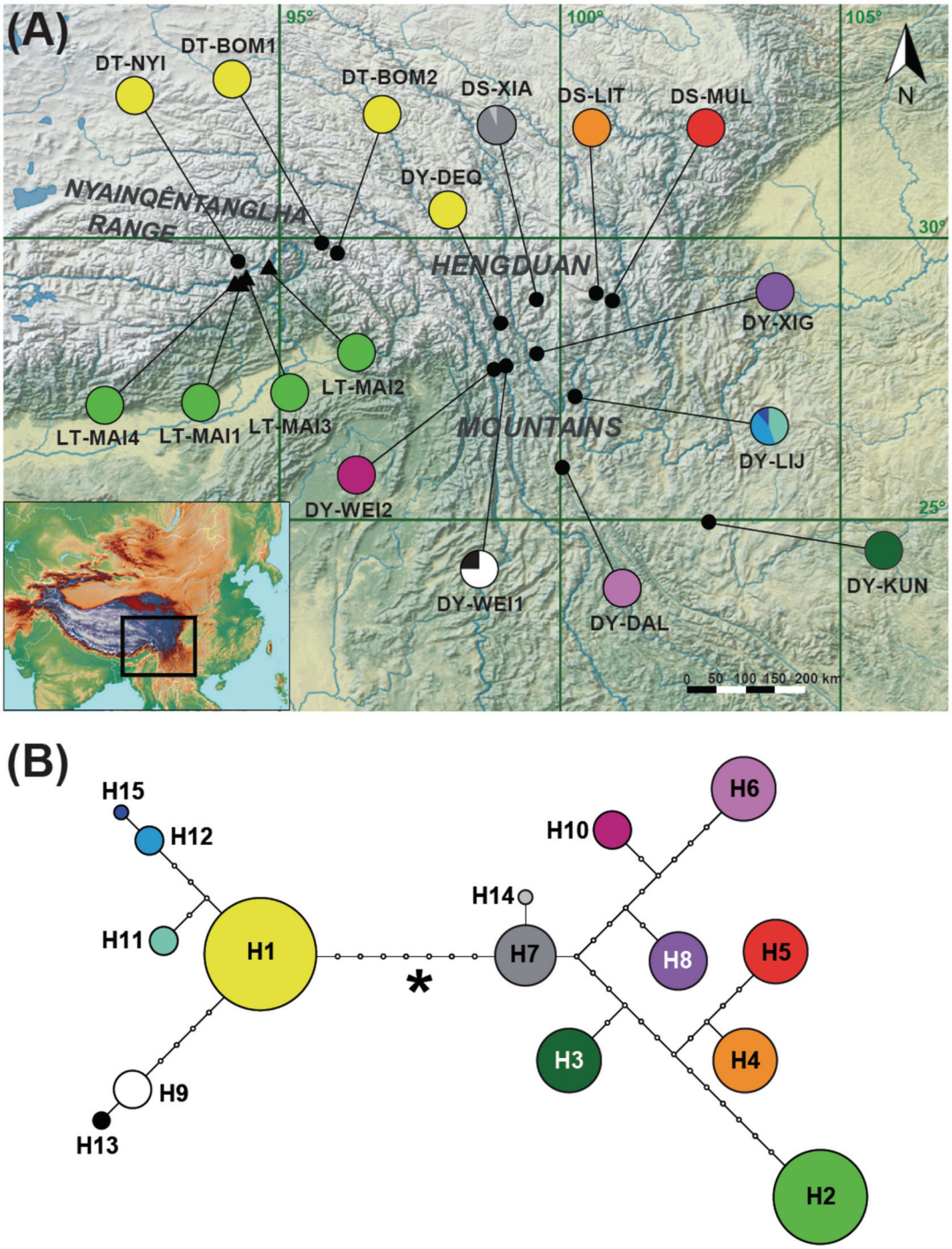

Fig. 2. Majority-rule consensus tree from a Bayesian analysis of the concatenate sequences of plastid DNA of *Paeonia* subct *Delavayanae* with Bayesian posterior probabilities indicated below branches and bootstrap values above branches. Supported branches are indicated in bold.

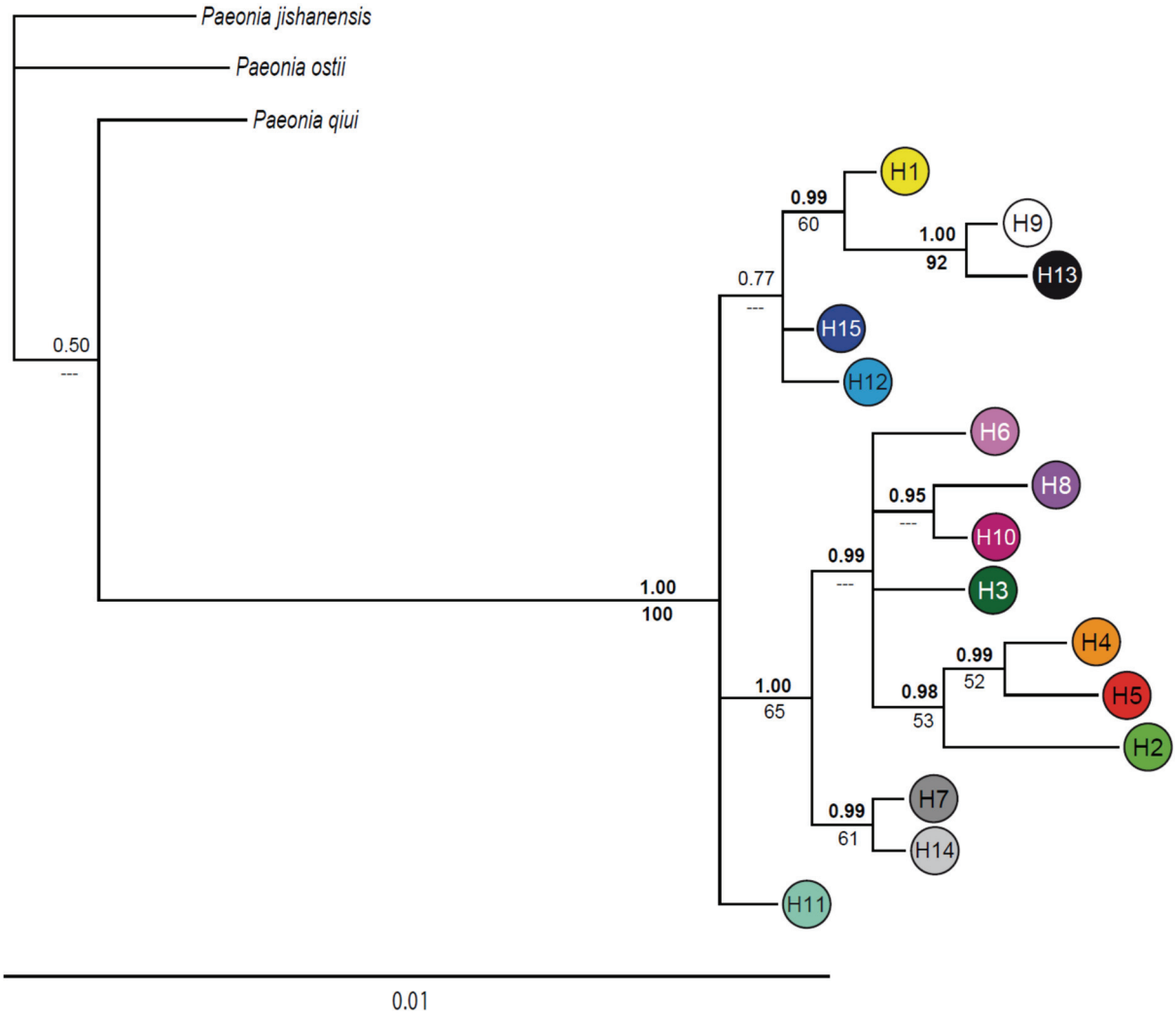

Fig. 3. Unweighted pair-group method using arithmetic averages (UPGMA) dendrogram using Rogers' (1972) distance (D_R) of 17 populations of *Paeonia* subsect. *Delavayanae* based on nSSR data. Numbers above branches represent bootstrap support for 1000 replicates; only values equal to or greater than 50% are given. *Paeonia delavayi* populations are in bold, those of *P. ludlowii* in italics.

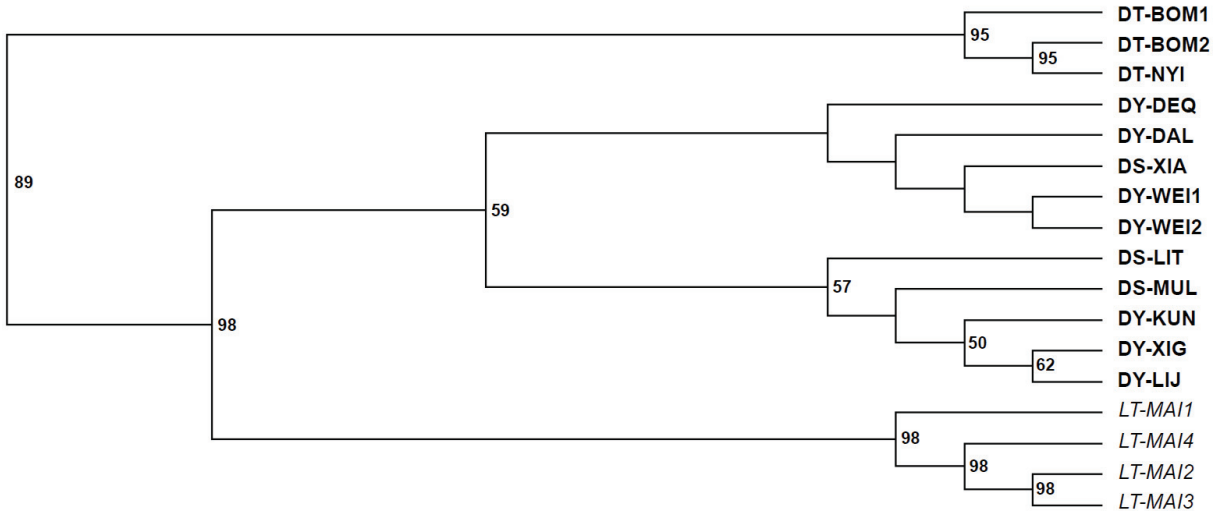

Fig. 4. Principal coordinate analysis (PCoA) of 17 populations of *Paeonia* subsect. *Delavayanae* based on nSSR, using codominant genetic distances. *Paeonia delavayi* populations are in bold, those of *P. ludlowii* in italics.

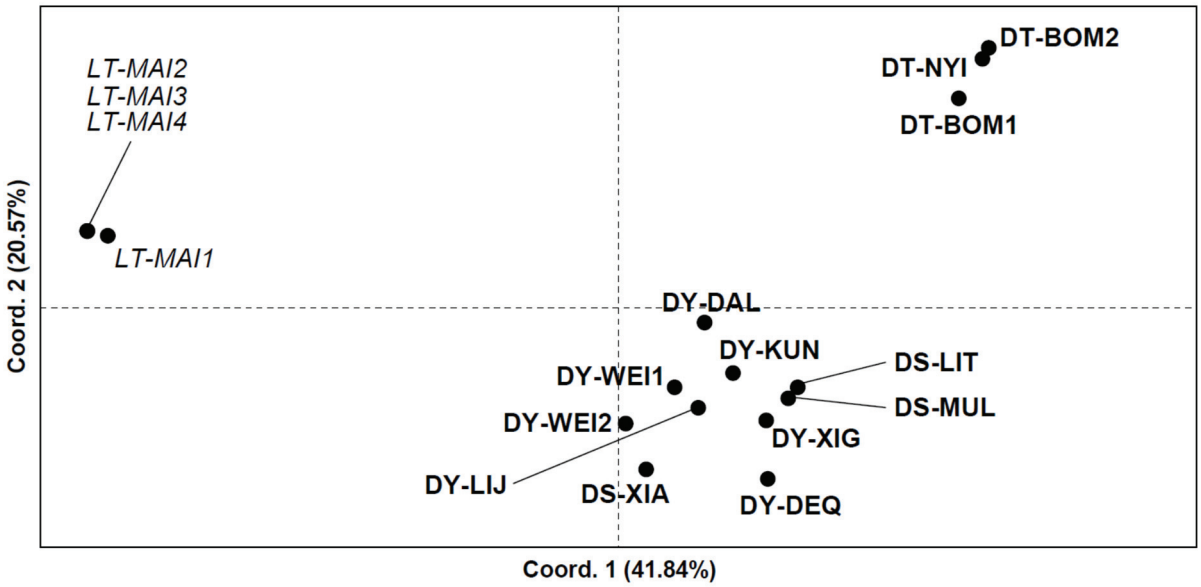

Fig. 5. Results of Structure analysis for all individuals of *Paeonia* subsect. *Delavayanae* studied, based on nSSR data. (A) The most likely *K* was estimated by choosing the smallest *K* after the log probability of data [ln Pr(*X*|*K*)] values reached a plateau (Pritchard et al., 2010), and (B) the Δ*K* statistic of Evanno et al. (2005). (C) Assignation of individuals to genetic clusters at *K* = 13.

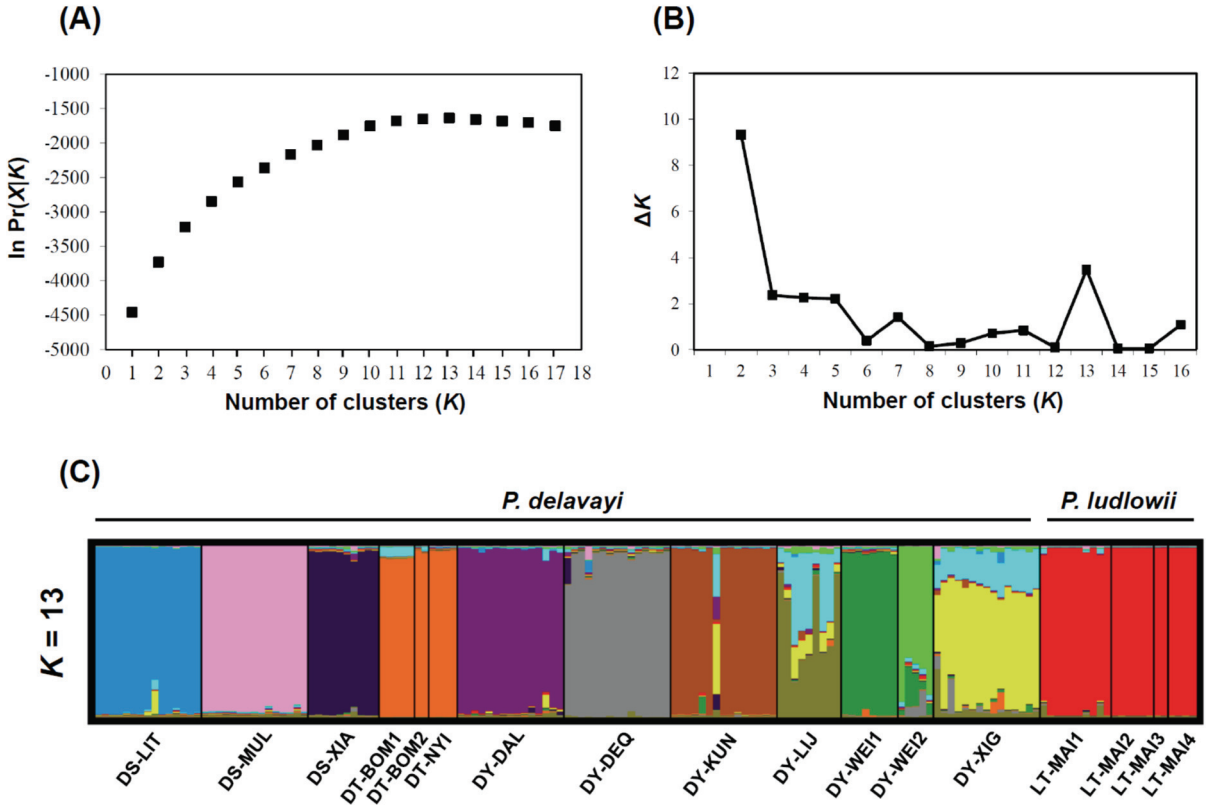

Fig. 6. Schematic representation of the first nine barriers detected in *Paeonia* subsect. *Delavayanae* using the program Barrier based on nSSR (A) and plastid DNA (B). For the nSSR, results are based on 1000 bootstrap matrices of Nei et al. (1983) genetic distance (D_A). Numbers indicate bootstrap support (after nine barriers). The location of populations is indicated by dots (full dots, *P. delavayi*; empty dots, *P. ludlovii*) whereas the polygons result from the Voronoi tessellation.

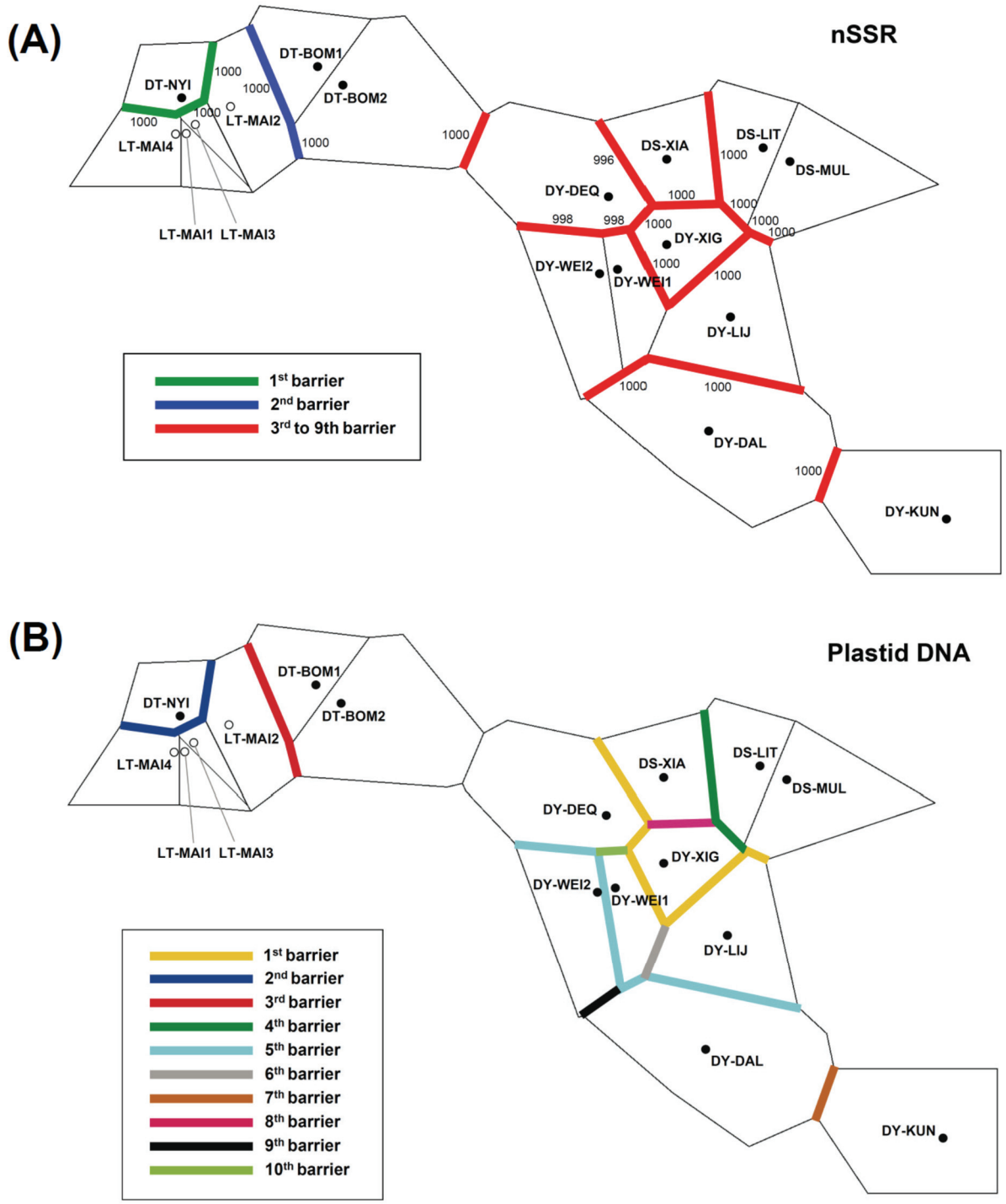

Fig. 7. Comparison of potential distributions as probability of occurrence for *Paeonia delavayi*, *P. ludlowii*, and *P. delavayi* + *P. ludlowii* using MaxEnt (Phillips et al., 2006), at the present time and at three climatic scenarios of the Last Glacial Maximum (LGM, ca. 21,000 years BP). The maximum training sensitivity plus specificity logistic threshold has been used to discriminate between suitable (gray-shaded) and unsuitable habitat. The darker color indicates a higher probability of occurrence. Black circles and black squares represent extant occurrence points of *P. delavayi* and *P. ludlowii*, respectively.

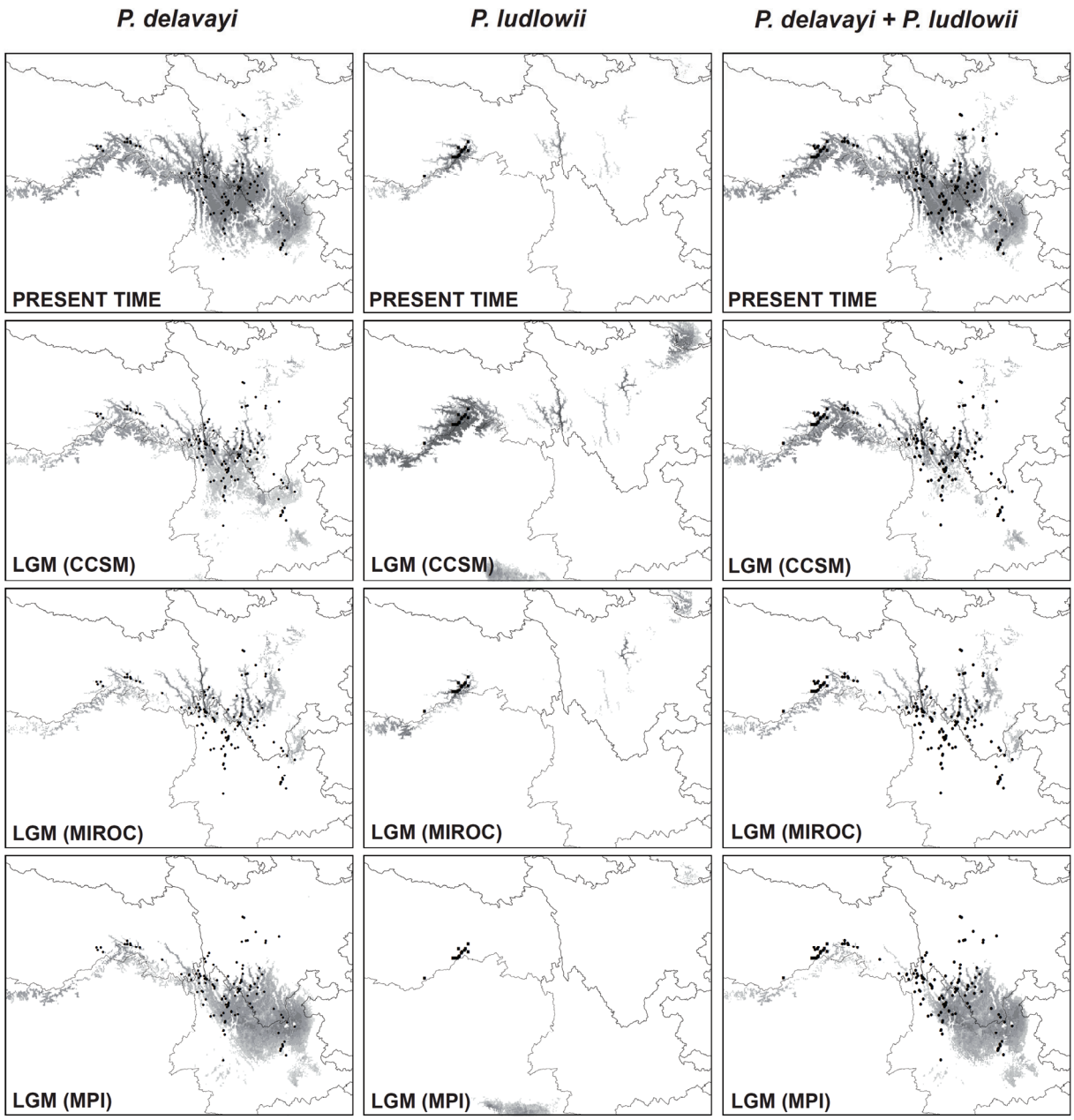

Fig. 8. Reconstruction of the extension of the Last Glacial Maximum (LGM, ca. 21,000 years BP) glaciers and ice caps in the study area, following the original map of Li et al. (1991). The value of expected heterozygosity (H_e; red bar) and the number of alleles (blue bar) are given for each population. In light blue, total number of alleles (TA), in dark blue, number of private aleles (PA).

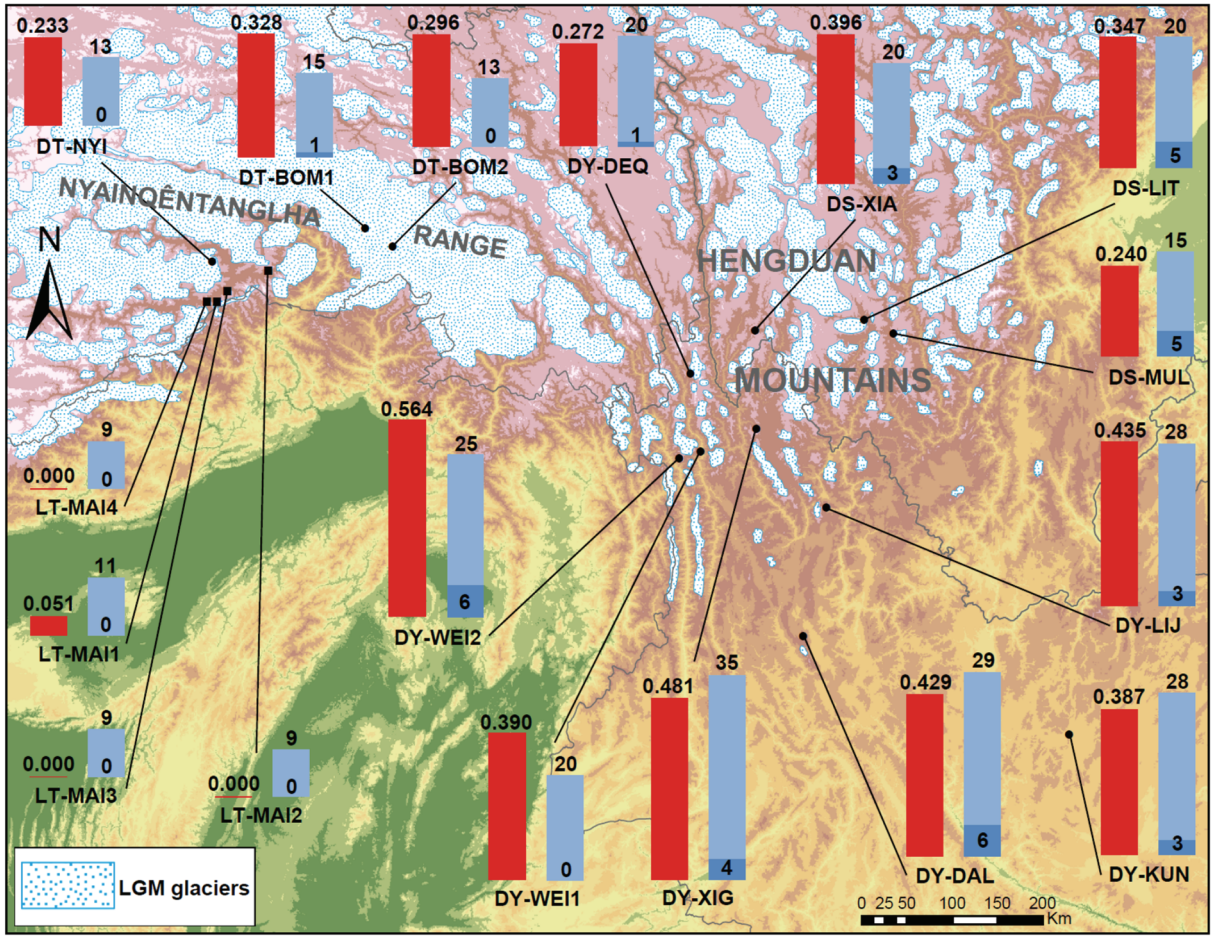

TABLES

Table 1. Details of sampled populations of *Paeonia delavayi* and *P. ludlowii*. *N* = number of individuals investigated. * The population abbreviation consists of the first letter of species epithet, the first letter of province, and the first tree letters of county.

Population abbreviation*	Locality (village, country, province)	Latitude (N), longitude (E)	Altitude (m)	Plastid DNA (*N*)	nSSR (*N*)
P. delavayi					
DS-LIT	Maiwa, Litang, Sichuan	29º01′N, 100º38′E	3153	15	15
DS-MUL	Shawan, Muli, Sichuan	28º54′N, 100º55′E	3486	15	15
DS-XIA	Baiyi, Xiangcheng, Sichuan	28º54′N, 99º34′E	3175	15	10
DT-BOM1	Guxiang, Bomi, Tibet	29º55′N, 95º45′E	2600	5	5
DT-BOM2	Sumzom, Bomi, Tibet	29º44′N, 96º01′E	3100	2	2
DT-NYI	Zanba, Nyingchi, Tibet	29º35′N, 94º15′E	3000	4	4
DY-DAL	Cangshan, Dali, Yunnan	25º55′N, 100º02′E	2564	15	15
DY-DEQ	Mingyong, Dêqên, Yunnan	28º29′N, 98º56′E	2850	15	15
DY-KUN	Xishan, Kunming, Yunnan	24º57′N, 102º38′E	2000	15	15
DY-LIJ	Maoniuping, Lijiang,Yunnan	27º11′N, 100º16′E	2690	9	9
DY-WEI1	Duoduo, Weixi, Yunnan	27º42′N, 99º02′E	3483	8	8
DY-WEI2	Laboluo, Weixi, Yunnan	27º40′N, 98º50′E	3720	6	5
DY-XIG	Hala, Xianggelila, Yunnan	27º57′N, 99º35′E	3200–3300	13	15
P. ludlowii					
LT-MAI1	Zhare, Mainling, Tibet	29º12′N, 94º18′E	2980	10	10
LT-MAI2	Jinxuega, Mainling, Tibet	29º30′N, 94º48′E	2900	6	6
LT-MAI3	Gangga, Mainling, Tibet	29º18′N, 94º24′E	2900	2	2
LT-MAI4	Between Gangga and Mainling, Mainling, Tibet	29º12′N, 94º12′E	3000	4	4
Total				159	155

Table 2. Genetic diversity parameters and fixation index in 17 populations of *Paeonia* subsect. *Delavayanae* based on nSSR. P_{99} = percentage of polymorphic loci when the most common allele had a frequency of < 0.99; *A* = mean number of alleles per locus; *AR* = allelic richness (adjusted for a sample size of two individuals); *TA* = total number of alleles; *PA* = number of private alleles; *RA* = number of rare alleles (those occurring at frequencies below 0.05); H_o = observed heterozygosity; H_e = aunbiased expected heterozygosity or Nei's (1978) gene diversity; F_{IS} = fixation index. SE = standard error.

Population symbol	P_{99} (%)	*A*	*AR*	*TA/PA/RA*	H_o	H_e (SE)	F_{IS}[1]	IAM[2]		SMM[2]	
P. delavayi											
DS-LIT	88.9	2.222	1.675	20/5/1	0.283	0.347 (0.071)	0.193*	0.111	**0.020**	0.414	0.191
DS-MUL	55.6	1.667	1.439	15/5/0	0.346	0.240 (0.085)	**–0.469*****	0.146	**0.031**	0.214	**0.047**
DS-XIA	88.9	2.222	1.770	20/3/0	0.279	0.396 (0.079)	0.310*	**0.026**	**0.020**	**0.040**	0.098
DT-BOM1	66.7	1.667	1.577	15/1/0	0.422	0.328 (0.085)	–0.333^{ns}	—	—	—	—
DT-BOM2	44.4	1.444	1.444	13/0/0	0.333	0.296 (0.117)	–0.200^{ns}	—	—	—	—
DT-NYI	44.4	1.444	1.405	13/0/0	0.176	0.233 (0.093)	0.296^{ns}	—	—	—	—
DY-DAL	77.8	3.222	1.926	29/6/6	0.360	0.429 (0.094)	0.165*	0.579	0.289	0.587	0.594
DY-DEQ	88.9	2.222	1.505	20/1/3	0.210	0.272 (0.083)	0.320^{ns}	0.529	0.578	0.340	0.844
DY-KUN	77.8	3.111	1.803	28/3/7	0.444	0.387 (0.087)	–0.153*	0.602	0.531	0.325	0.656
DY-LIJ	88.9	3.111	1.932	28/3/0	0.332	0.435 (0.080)	0.252**	—	—	—	—
DY-WEI1	88.9	2.222	1.760	20/0/0	0.389	0.390 (0.078)	0.004^{ns}	—	—	—	—
DY-WEI2	88.9	2.778	2.186	25/6/0	0.367	0.564 (0.085)	0.392**	—	—	—	—
DY-XIG	77.8	3.889	2.077	35/4/10	0.399	0.481 (0.107)	0.171^{ns}	0.319	0.344	0.607	0.766
Mean (95% CI)	75.2	2.402	1.731	21.6/2.8/2.1	0.334	0.369	0.061 (–0.065, 0.190)				
P. ludlowii											
LT-MAI1	22.2	1.222	1.097	11/0/0	0.056	0.051 (0.034)	–0.098^{ns}	0.341	1.000	0.217	1.000
LT-MAI2	0.0	1.000	1.000	9/0/0	0.000	0.000 (0.000)	—	—	—	—	—
LT-MAI3	0.0	1.000	1.000	9/0/0	0.000	0.000 (0.000)	—	—	—	—	—
LT-MAI4	0.0	1.000	1.000	9/0/0	0.000	0.000 (0.000)	—	—	—	—	—
Mean (95% CI)	5.6	1.056	1.024	9.5/0/0	0.014	0.013	–0.050				

								(–0.067, –0.021)
Mean	*P.*	subsec.	58.8	2.085	1.564	18.8/2.2/1.6	0.259	0.285 (0.023)	0.066
Delavayanae (95% CI)									(–0.056, 0.195)

[1] **P* < 0.05; ***P* < 0.01; ***P* < 0.001; [ns]not significant; in bold, significant values after the Bonferroni correction.

[2] Numbers reported are *P* values of sign tests (left) and Wilcoxon signed-rank tests (right) under IAM (infinite allele model), and SMM (stepwise mutation model) conducted using the program Bottleneck. Significant *P* values (at the 0.05 level) are boldfaced.

Table 3. Analysis of molecular variance (AMOVA) of *Paeonia* subsect. *Delavayanae* based on nSSR and plastid DNA variation. *df* = degrees of freedom; SS = sum of squares; Vc = variance component. *$P < 0.05$; **$P < 0.01$; **$P < 0.001$; ^{ns}not significant.

Taxon/source	nSSR				plastid DNA			
	df	SS	Vc	%	*df*	SS	Vc	%
P. delavayi + *P. ludlowii*								
Among taxa	1	175.805	2.017	40.3***	1	158.699	3.264	42.02***
Among populations within taxa	15	401.649	1.395	27.9***	15	618.048	4.433	57.08***
Within populations	293	465.285	1.588	31.8***	142	9.989	0.070	0.91***
P. delavayi (no regional categories)								
Among populations	12	401.295	1.575	46.4***	12	618.048	4.966	98.40**
Within populations	253	460.935	1.822	53.6 ^{ns}	124	9.989	0.081	1.60**
P. ludlowii (no regional categories)								
Among populations	3	0.355	0.001	0.9 ^{ns}	3	0.000	0.000	—
Within populations	40	4.350	0.109	99.1^{ns}	18	0.000	0.000	—
Paeonia subsect. *Delavayanae*								
Among 3 genetic clusters[1]	2	230.119	1.773	38.5***	—	—	—	—
Among populations within clusters	14	347.335	1.245	27.0***	—	—	—	—
Within populations	293	465.285	1.588	34.5***	—	—	—	—

[1] Genetic clusters delimited according to both the UPGMA dendrograms and PCoA.

Table 4. Pairwise comparisons showing differentiation between populations of *Paeonia* subsect. *Delavayanae* using Wright's (1965) F_{ST}, based on nSSR variation. *$P < 0.05$; **$P < 0.01$; **$P < 0.001$; ^{ns}not significant; NA, not applicable; in bold, significant values after the Bonferroni correction.

	DS-LIT	DS-MUL	DS-XIA	DT-BOM1	DT-BOM2	DT-NYI	DY-DAL	DY-DEQ	DY-KUN	DY-LIJ	DY-WEI1	DY-WEI2	DY-XIG	LT-MAI1	LT-MAI2	LT-MAI3	LT-MAI4
DS-LIT	—																
DS-MUL	**0.602*****	—															
DS-XIA	0.576***	**0.520*****	—														
DT-BOM1	0.622**	0.672**	0.587**	—													
DT-BOM2	0.599^{ns}	0.683^{ns}	0.580 ^{ns}	0.310^{ns}	—												
DT-NYI	0.616**	0.687**	0.620*	0.432^{ns}	0.044^{ns}	—											
DY-DAL	**0.530*****	**0.534*****	**0.382*****	0.490**	0.439^{ns}	0.496**	—										
DY-DEQ	**0.629*****	**0.680*****	0.494***	0.671**	0.691^{ns}	0.728**	**0.464*****	—									
DY-KUN	**0.540*****	**0.546*****	**0.495*****	0.574**	0.576^{ns}	0.604**	**0.507*****	**0.573*****	—								
DY-LIJ	0.487***	**0.381*****	0.321***	0.527*	0.481^{ns}	0.557*	**0.409*****	**0.557*****	0.422***	—							
DY-WEI1	0.562***	0.573***	0.377**	0.517*	0.552^{ns}	0.588*	0.424***	0.528***	0.481***	0.422**	—						
DY-WEI2	0.501**	0.582**	0.330**	0.464^{ns}	0.439^{ns}	0.521*	0.270**	0.373**	0.441**	0.380**	0.170*	—					
DY-XIG	**0.437*****	**0.497*****	**0.361*****	0.505**	0.477^{ns}	0.536**	**0.421*****	**0.472*****	**0.368*****	0.213***	0.372***	0.332**	—				
LT-MAI1	0.777***	0.824***	0.718**	0.856**	0.911^{ns}	0.902*	**0.664*****	**0.831*****	**0.736*****	0.717**	0.738**	0.708**	0.688***	—			
LT-MAI2	0.763**	0.825**	0.702**	0.855*	0.936^{ns}	0.914*	0.646**	0.826**	0.720**	0.699**	0.720**	0.676*	0.668**	0.049^{ns}	—		
LT-MAI3	0.705^{ns}	0.786^{ns}	0.595^{ns}	0.778^{ns}	0.861^{ns}	0.836^{ns}	0.568^{ns}	0.754^{ns}	0.661^{ns}	0.587^{ns}	0.620^{ns}	0.485^{ns}	0.583^{ns}	–0.062^{ns}	NA	—	
LT-MAI4	0.739*	0.808*	0.661*	0.825^{ns}	0.913^{ns}	0.888^{ns}	0.615*	0.802*	0.695*	0.655*	0.680*	0.608^{ns}	0.635*	0.016^{ns}	NA	NA	—

Supplementary Material

Population genetic dynamics of Himalayan-Hengduan tree peonies, *Paeonia* subsect. *Delavayanae*

Jin-Mei Zhang, Jordi López-Pujol, Xun Gong, Hua-Feng Wang, Roser Vilatersana and Shi-Liang Zhou

Supplementary Text 1. Extended material of Ecological niche modeling methodology.

Ecological niche modeling (ENM) was performed to evaluate the potential distribution of *Paeonia delavayi*, *P. ludlowii*, and *P. delavayi* + *P. ludlowii*. We employed the maximum entropy algorithm, as implemented in MaxEnt v.3.3 (Phillips et al., 2006). The current distribution information for both species was obtained from the sampling sites (Table 1), literature (e.g., Hong, 2010), and specimens deposited in the main Chinese herbaria (through the Chinese Virtual Herbarium platform; www.cvh.ac.cn). After removing duplicate records within each pixel (2.5 arc-min, *ca*. 5 km), we obtained a total of 119 presence records of *P. delavayi* and 13 records of *P. ludlowii*. A set of 19 bioclimatic variables at 2.5 arc-min resolution covering the distribution range (and neighboring areas) for both species under current conditions (1950–2000) were downloaded from the WorldClim website (www.worldclim.org; Hijmans et al., 2005). Although finer resolutions are available (30 arc-sec), these may not be appropriate given uncertainties associated with geo-referencing approximate localities (a common situation for old herbarium records in China, especially for remote areas) or with geo-reference errors. After a correlation analysis in a random sample of 1000 points within the study area, we selected a smaller set of eight (relatively) uncorrelated variables: mean diurnal range (bio2), isothermality (bio3), temperature seasonality (bio4), mean temperature of the coldest quarter (bio11), annual precipitation (bio12), precipitation of the driest month (bio14), precipitation seasonality (bio15), and precipitation of the coldest quarter (bio19). The selection of variables from pairs or groups of highly correlated ($r \geq |0.9|$) ones was done on the basis of their relative contribution to the models (percent contribution, permutation importance, jackknife of regularized gaining train), making sure that the top most influential variables for the two species were selected.

The distribution model under current conditions was projected to the Last Glacial Maximum (LGM, *ca*. 21,000 yr BP) using palaeoclimatic layers simulated by the Community Climate System Model version 4 (CCSM4; Gent et al., 2011), the Model for Interdisciplinary Research on Climate Earth System Model (MIROC-ESM; Watanabe et al., 2011), and the New Earth System Model of Max Planck Institute for Meteorology (MPI-ESM; http://www.mpimet.mpg.de/en/science/models/mpi-esm/). For the models with a considerable number of occurrences (*P. delavayi* and *P. delavayi* + *P. ludlowii*) 20 replicates of MaxEnt (using the subsample method) were run, and model performance was assessed using the area

under the curve (AUC) of the receiver operating characteristic (ROC) plot with 25% of the localities randomly selected to test the model. AUC scores range between 0.5 (randomness) and 1 (exact match), and a value above 0.9 is considered a good performance of the model (Swets, 1988). Given the low number of occurrences for *P. ludlowii* (13), we used a methodology based on a jackknife (or 'leave-one-out') procedure to test the model (Pearson et al., 2007). With this procedure the model is built (or 'trained') using n–1 occurrences, and tested using the discarded locality. Following the recommendation of Pearson et al. (2007), the Lowest Presence Threshold (LPT, also commonly referred as 'minimum training presence' in the MaxEnt terminology) was used as the cut-off value to decide whether the discarded locality is 'suitable' or 'unsuitable'. Performance of models for *P. ludlowii* was evaluated through success rate (percentage of right predictions) and statistical significance (a *P*-value computed across the set of jackknife predictions, which was done using the software provided by Pearson et al. (2007). To get the definitive model (that is, using all occurrence points) MaxEnt was run 20 times using the bootstrap method.

The MaxEnt jackknife analysis was used to evaluate the relative importance of the eight bioclimatic variables employed based on their gain values when used in isolation. To convert the continuous value projection to a binary presence/absence distribution, we applied the maximum sensitivity plus specificity logistic threshold, which is very robust with all types of data (Liu et al., 2016). All ENM predictions were visualized in ArcGIS v. 10.2 (ESRI, Redlands, CA, USA). The suitable area (in km^2) for all models at each time slice was also calculated in ArcGIS. To estimate suitable area gains or losses (or unchanged areas) for the LGM scenarios with respect to the present, binary output maps were overlapped with the Intersect Tool of ArcGIS.

Niche similarity between *P. delavayi* and *P. ludlowii* was measured through two niche overlap indices, Hellinger-derived *I* and Schoener's *D*. These metrics are implemented in the software ENMTools v.1.4.3 (Warren et al., 2010). The *I* and *D* values range from 0 (when the two species show completely discordant ENMs) to 1 (complete niche overlap). Two quantitative tests of niche similarity that are also implemented in ENMTools were further used. The 'niche identity test' determines whether two ENMs are identical by comparing the empirical *I* and *D* values to those generated from a number of pseudoreplicated datasets that are obtained by pooling all the occurrences of the two species and randomly splitting them into two new groups. The 'background test' determines whether ENMs are more similar (or less similar) than would be expected given the underlying environmental differences between the regions in which the entities to compare occur. A null distribution of *I* and *D* values was generated by comparing the actual occurrence records of *P. delavayi* with a set of randomly simulated occurrences within the range of *P. ludlowii*, and *vice versa*. Niche conservatism (niches more similar than expected) or divergence (niches more different than expected) can be interpreted when the empirical niche overlap values are significantly larger and smaller than those of the null hypothesis, respectively. Backgrounds were delimited by creating a buffer zone of 20 km around the occurrence points of each species, with the aid of the specific tools included in ArcGIS. For both tests, null distributions were generated from 100 pseudoreplicates. Finally, we estimated the niche breadth for each species by calculating the inverse concentration statistic of Levins (1968), as implemented in ENMTools; values range from 0 (only one pixel shows suitability greater than zero) to 1 (all pixels equally suitable).

References

Gent, P.R., Danabasoglu, G., Donner, L.M., Holland, M.M., Hunke, E.C., Jayne, S.R., Lawrence, D.M., Neale, R.B., Rasch, P.J., Vertenstein, M., Worley, P.H., Yang, Z-L., Zhang, M., 2011. The community climate system model version 4. J. Climate 24, 4973–4991.

Hijmans, R.J., Camerson, S.E., Parra, J.L., Jone, P.G., Javis, A., 2005. Very high solution interpolated climate surfaces for global land areas. Int. J. Climatol. 25, 1965–1978.

Hong, D.-Y., 2010. Peonies of the world. Taxonomy and phytogeography. Royal Botanical Gardens Kew-Missouri Botanical Garden, London-St. Louis.

Levins, R., 1968. Evolution in changing environments. Princeton University Press, Princeton.

Liu, C., Newell, G., White, M., 2016. On the selection of thresholds for predicting species occurrence with presence-only data. Ecol. Evol. 6, 337–348.

Pearson, R.G., Raxworthy, C.J., Nakamura, M., Peterson, A.T., 2007. Predicting species distributions from small numbers of occurrence records: a test case using cryptic geckos in Madagascar. J. Biogeogr. 34, 102–117.

Phillips, S.J., Anderson, R.P., Schapire, R.E., 2006. Maximum entropy modeling of species geographic distributions. Ecol. Model. 190, 231–259.

Swets, J.A., 1988. Measuring the accuracy of diagnostic systems. Science 240, 1285–1293.

Warren, D.L., Glor, R.E., Turelli, M., 2010. ENMTools: a toolbox for comparative studies of environmental niche models. Ecography 33, 607–611.

Watanabe, S., Hajima, T., Sudo, K., Nagashima, T., Takemura, T., Okajima, H., Nozawa, T., Kawase, H., Abe, M., Yokohata, T., Ise, T., Sato, H., Kato, E., Takata, K., Emori, S., Kawamiya, M., 2011. MIROC-ESM: model description and basic results of CMIP5–20c3m experiments. Geosci. Model Dev. 4, 845–872.

Fig. S1. Unweighted pair-group method using arithmetic averages (UPGMA) dendrogram using Nei's (1972) standard genetic distance (D_S), based on nSSR variation. Numbers above branches represent bootstrap support for 1000 replicates; only values equal to or greater than 50% are given. *Paeonia delavayi* populations are in bold, those of *P. ludlowii* in italics.

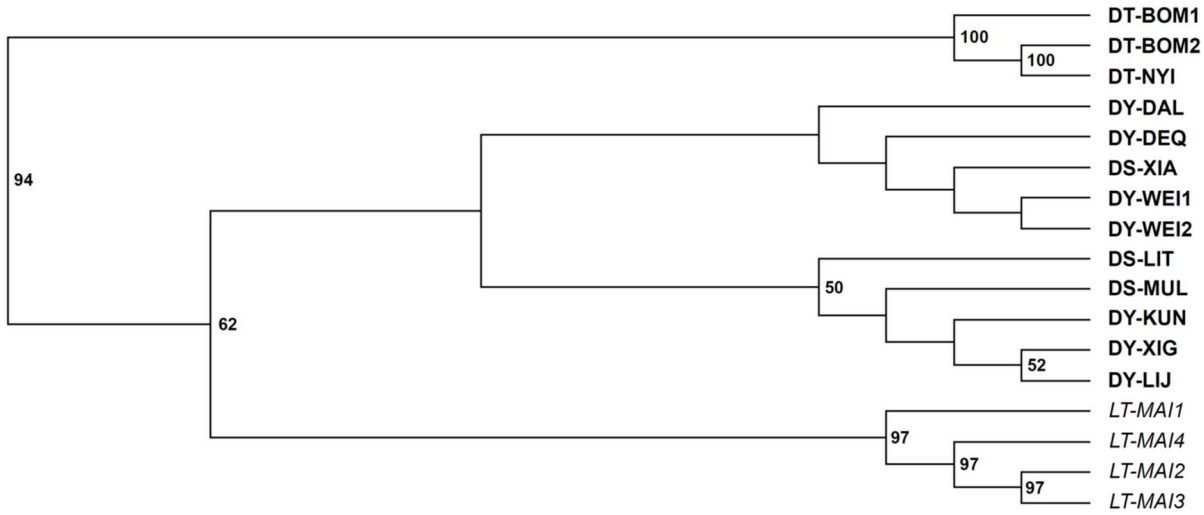

Reference

Nei, M., 1972. Genetic distance between populations. Am. Nat. 106, 289–291.

Fig. S2. Results of Structure analysis for all individuals of *Paeonia* subsect. *Delavayanae* studied, based on nSSR data. Assignation of individuals to genetic clusters from $K = 2$ to $K = 13$.

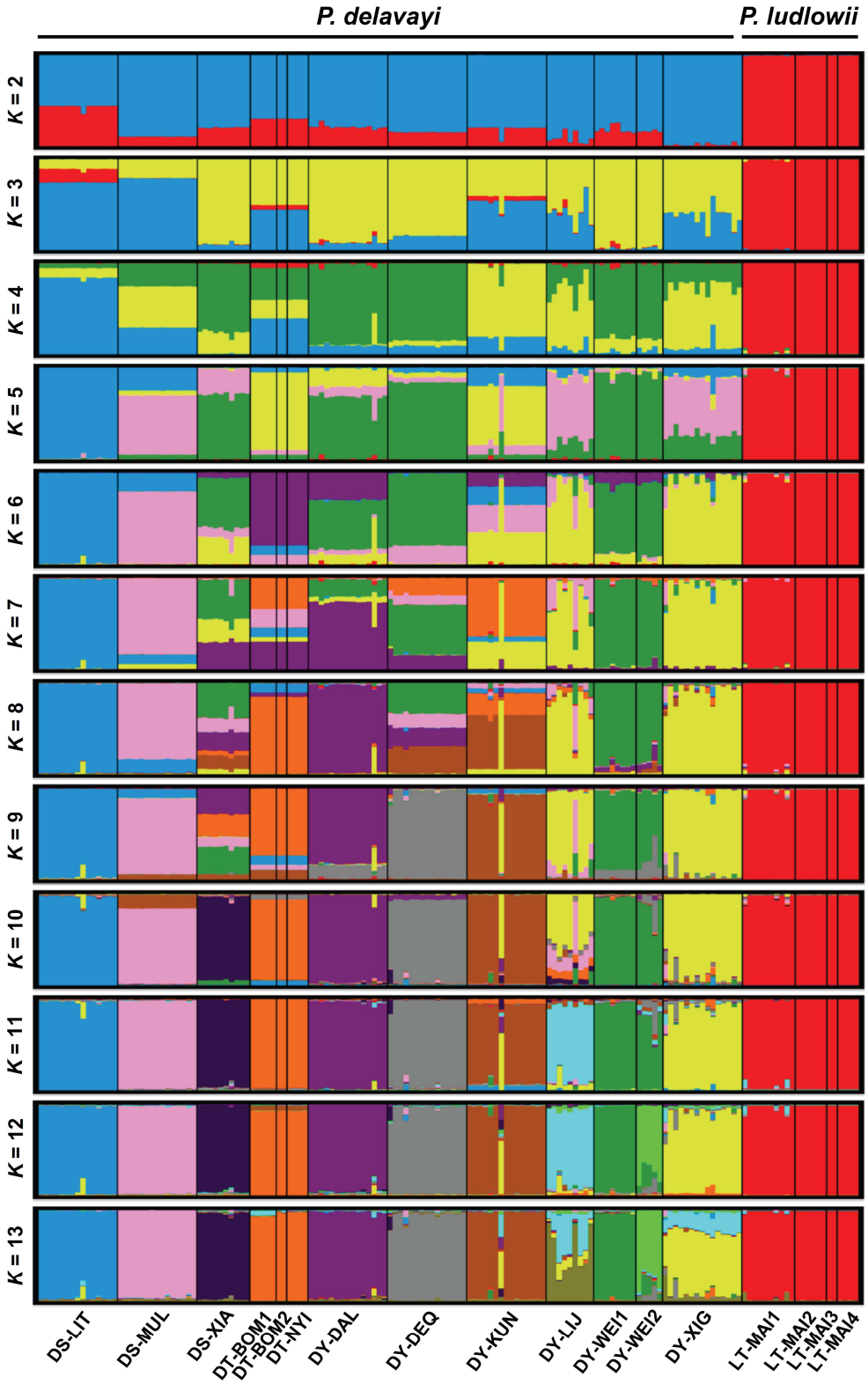

Fig. S3. Results of Structure analysis for all individuals of *Paeonia* subsect. *Delavayanae* studied, based on nSSR data. Representation of the 20 runs at $K = 2$.

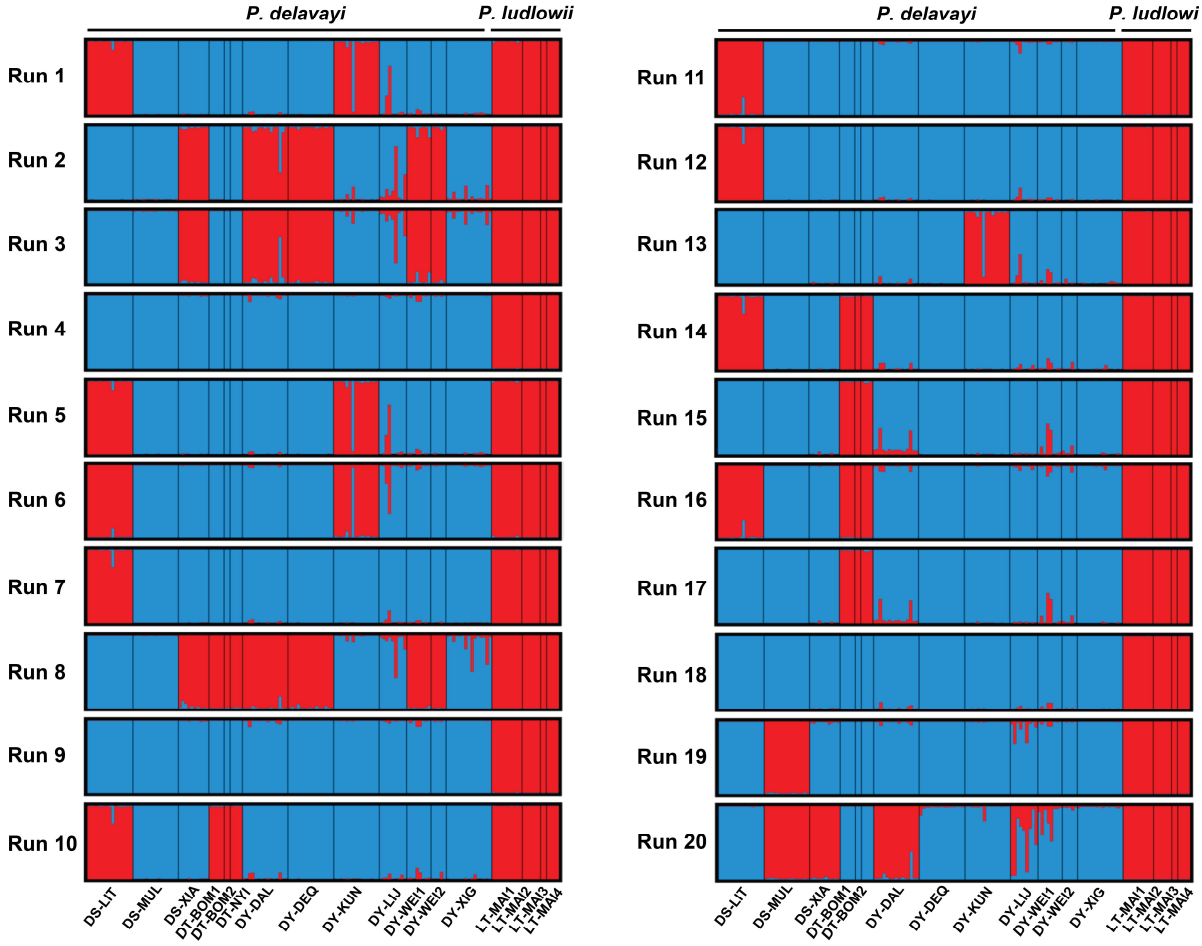

Fig. S4. Observed and expected mismatch distribution under constant population size of *Paeonia* subsect. *Delavayanae*.

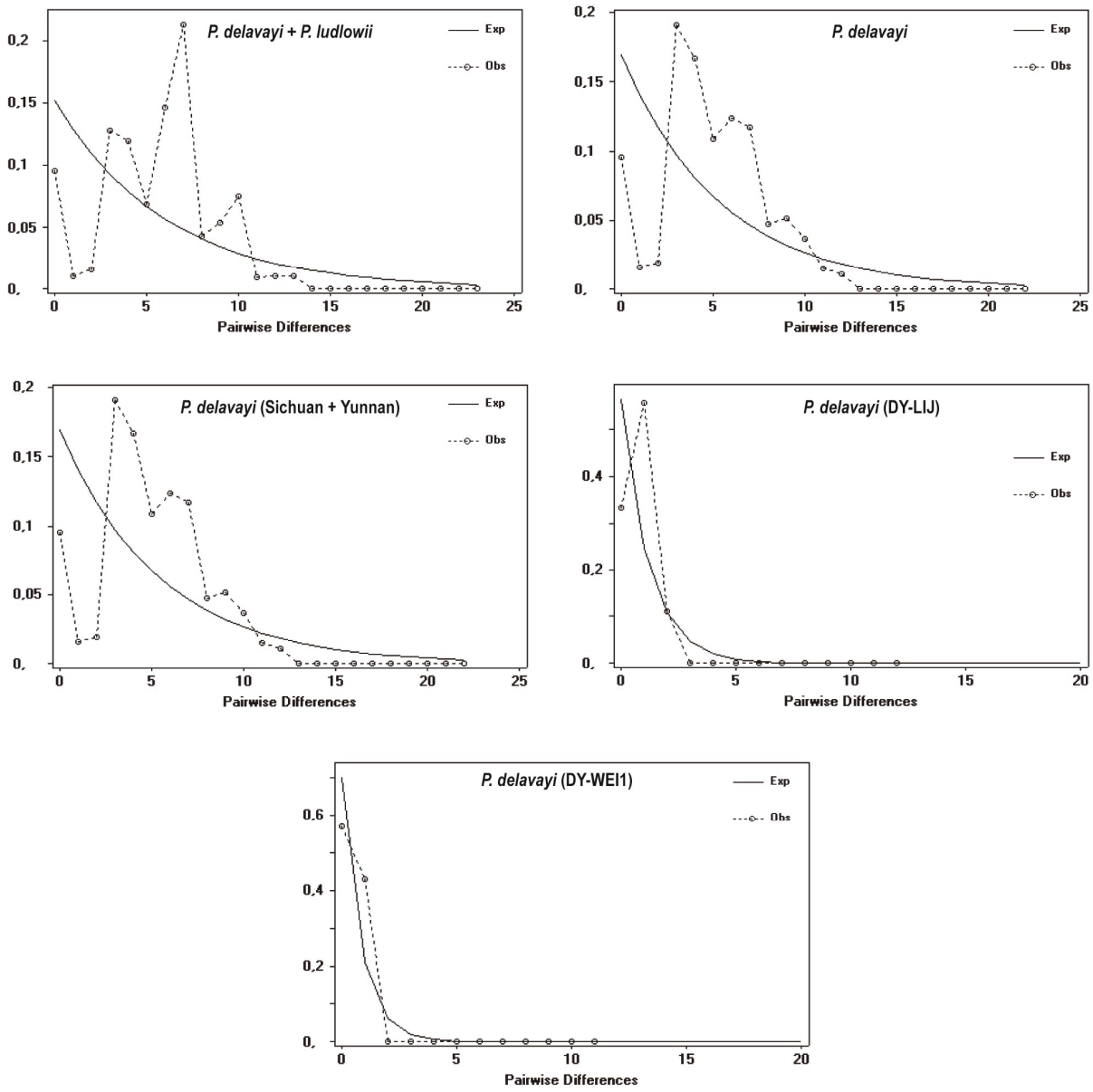

Fig. S5. Comparison of potential distributions for *Paeonia delavayi*, *P. ludlowii*, and *P. delavayi* + *P. ludlowii* between the present time and each of the three climatic scenarios assayed for the Last Glacial Maximum (LGM, ca. 21,000 years BP). In gray, no change between present and past climatic scenarios; in red, LGM contraction areas (that is, areas gained in the present compared to the LGM); in green, LGM expansion areas.

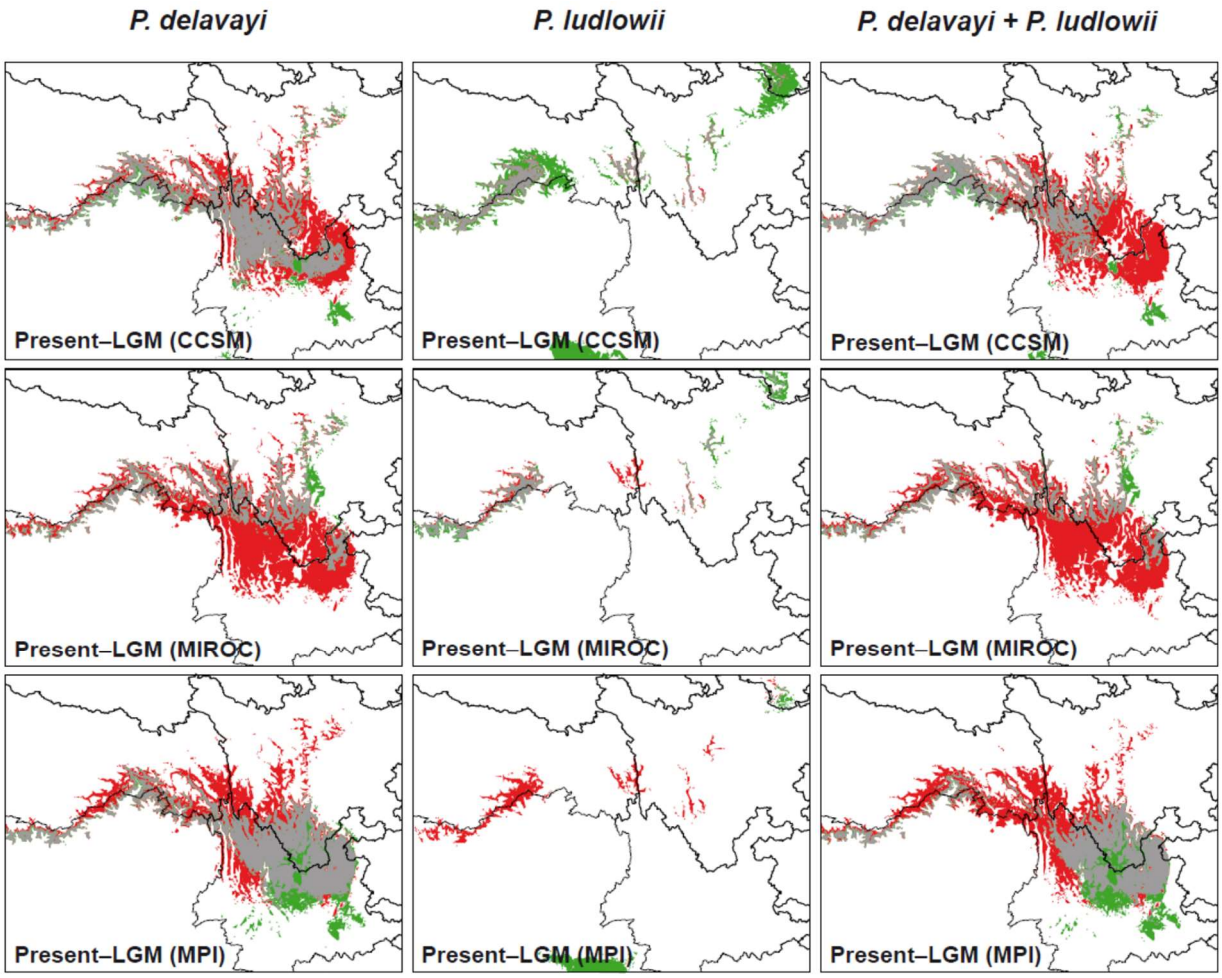

Fig. S6. Results of the two tests of niche similarity between *Paeonia delavayi* and *P. ludlowii* as obtained using ENMTools. (A) and (B), niche identity tests between both species based on Hellinger-derived *I* and Schoener's *D*, respectively; (C) and (D), background tests between *P. delavayi* occurrences and *P. ludlowii* background based on *I* and *D*, respectively; (E) and (F), background tests between *P. ludlowii* occurrences and *P. delavayi* background based on *I* and *D*, respectively. The arrows represent the observed niche overlap between ENMs (*I* = 0.569 and *D* = 0. 307), whereas the histograms are those expected under the null hypotheses.

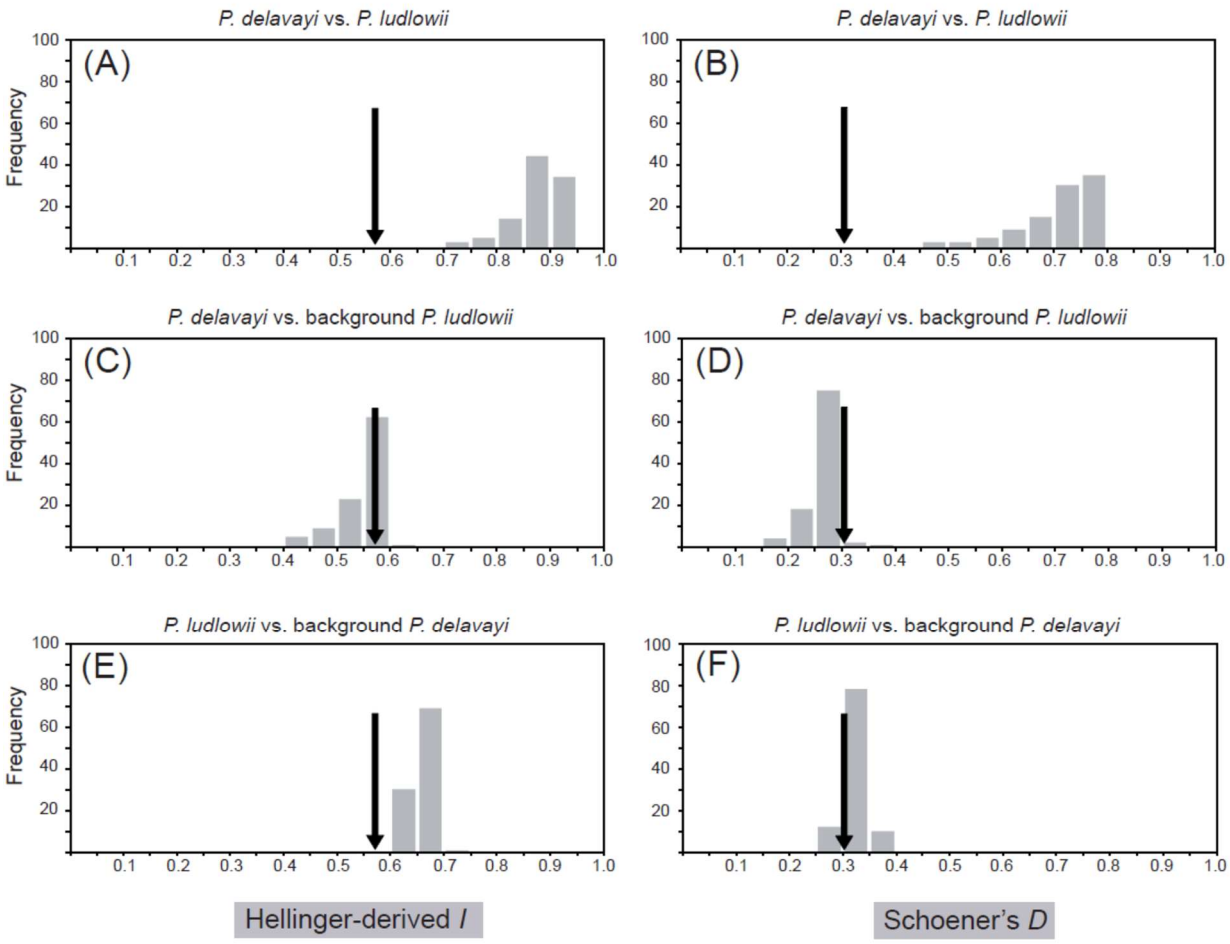

Table S1. Localities and voucher information for the population studied, and GenBank accession numbers for the four plastid DNA regions studied of *Paeonia* subsect. *Delavayanae*.

Population abbreviation*	Locality (village, county, province)	Voucher	*psbA-trnH*	*rps16-trnQ*	*ndhF*	*ndhC-trnV(UAC)*
P. delavayi						
DS-LIT	Maiwa, Litang, Sichuan	WY06078-LTP (PE)	MH025548	MH025569	MH025590	MH025611
DS-MUL	Shawan, Muli, Sichuan	91035 (KUN)	MH025549	MH025570	MH025591	MH025612
DS-XIA	Baiyi, Xiangcheng, Sichuan	WY06074-XCP (PE)	MH025553-554	MH025574-575	MH025595-596	MH025616-617
DT-BOM1	Guxiang, Bomi, Tibet	H060015 (PE)	MH025538	MH025559	MH025580	MH025601
DT-BOM2	Sumzom, Bomi, Tibet	H060016 (PE)	MH025539	MH025560	MH025581	MH025602
DT-NYI	Zanba, Nyingchi, Tibet	H060012 (PE)	MH025541	MH025562	MH025583	MH025604
DY-DAL	Cangshan, Dali, Yunnan	91027 (KUN)	MH025542	MH025563	MH025584	MH025605
DY-DEQ	Yunnan, Dêqên, Mingyong	701 (PE)	MH025540	MH025561	MH025582	MH025603
DY-KUN	Xishan, Kunming, Yunnan	WH05 (PE)	MH025544	MH025565	MH025586	MH025607
DY-LIJ	Maoniuping, Lijiang,Yunnan	82101 (KUN)	MH025545-547	MH025566-568	MH025587-589	MH025608-610
DY-WEI1	Duoduo, Weixi, Yunnan	82410 (KUN)	MH025550-551	MH025571-572	MH025592-593	MH025613-614
DY-WEI2	Laboluo, Weixi, Yunnan	82507 (KUN)	MH025552	MH025573	MH025594	MH025615
DY-XIG	Hala, Xianggelila, Yunnan	R05 (PE)	MH025543	MH025564	MH025585	MH025606
P. ludlowii						
LT-MAI1	Zhare, Mainling, Tibet	H03072 (PE)	MH025556	MH025577	MH025598	MH025619
LT-MAI2	Jinxuega, Mainling, Tibet	H03082 (PE)	MH025558	MH025579	MH025600	MH025621
LT-MAI3	Gangga, Mainling, Tibet	H06013 (PE)	MH025557	MH025578	MH025599	MH025620

LT-MAI4	Between Gangga and Mainling, Mainling, Tibet	H06014 (PE)	MH025555	MH025576	MH025597	MH025618
Outgroups						
P. jishanensis		BOP001735	MH051894	MH051896	MH051899	MH051902
P. ostii		BOP001481	KJ946192	MH051897	MH051900	KJ945956
P. qiui		BOP001030	MH051895	MH051898	MH051901	MH051903

* The population abbreviation consists of the first letter of species epithet, the first letter of province, and the first tree letters of county.

Note: KUN = Herbarium of Kunming Institute of Botany, Chinese Academy of Sciences; PE = Herbarium of the Institute of Botany, Chinese Academy of Sciences.

Table S2. Plastid genes, primers designed and annealing temperatures (Ta) for each plastid DNA region used in this study. PCRs were performed using the following program: 94 °C for 4 min; 35 cycles of 94 °C for 30 s, Ta °C for 30 s, and 72 °C for 2 min; and with a final extension at 72 °C for 10 min.

Gene	Primer name	Sequence (5'–3')	Ta (°C)
*psb*A-*trn*H	26f	CGCGCATGGTGGATTCACAATCC	52
	475r	GTTATGCATGAACGTAATGCTC	
*rps*16-*trn*Q	6022f	CGTTGCTTTCTACCACATCG	58
	7383r	CTATTCGGAGGTTCGAATCC	
*ndh*C- *trn*V$^{(UAC)}$	51189f	CGGATTCGAAATTGTAACCAAGC	56
	52001r	TGAAAAACAAGGGTCCTTGGC	
*ndh*F	110492f	CAATTATTCGCCTATCAA	52
	111588r	GTCTCAATTGGGTTATATGATG	

Table S3. Repeat motifs, annealing temperatures (Ta), primer sequences and the range of alleles detected per locus for the nine nSSR studied loci of *Paeonia* subsect. *Delavayanae*. The PCRs were performed using the following program 3 min at 94 °C, followed by 25 cycles of 30 s at 94 °C, 30 s at Ta °C, and 45 s at 72 °C, with a final extension of 10 min at 72 °C.

Locus	Repeat motif	Primer sequences (5'–3')	Size (bp)	Ta (°C)
Jx02*	(TC)9	F: TTGGTTGGTGAAGGTGTT R: CTTCGATAACCGCAGGAGGAT	289–331	54
Jx05*	(CT)17	F: GCCACAAGAAAACAAAAACC R: CCTTCACCACTACTTCCCCAT	214–246	54
Jx17*	(TC)20	F: CAAACTACCTGAATGTTCGGCTC R: CATCAAATTACCAAAGAAATCCT	187–225	54
Jx27*	(TC)5	F: GTTATAGAACCACTGACAT R: TGAGAGACAAATAATCGTG	303–321	48
Pdel05**	(AG)15	F: CCAATGTGGAAAATGAGTT R: CAAGCACAAGATGTAAGAA	180–226	50
Pdel11**	(TGG)6	F: CTGCCATTTCTTGCCTTCTTTGT R: TCTACCCTGCCAACAGCACATAC	230–242	54
Pdel20	(TC)6	F: TATAAATGGGAAGCAGACTCAA R: TATACTCAGCCTCGAAAAGAAG	253–329	54
Pdel22	(AG)9	F: TCGCCCAACCTGTCGTGGAGAT R: TTGAATAGAGCGGAATGGAAAA	300–328	54
Pdel35	(GA)10	F: ATGTCACCGAAAGTTGTGC R: AAAGCCTGGTGCAGTTATT	293–313	54

*Wang et al. 2009; **Zhang et al. 2011

References

Wang, J.X., Xia, T., Zhang, J.M., Zhou, S.L., 2009. Isolation and characterization of fourteen microsatellites from a tree peony (*Paeonia suffruticosa*). Conserv. Genet. 10, 1029–1031.

Zhang, J., Liu, J., Sun, H., Yu, J., Wang, J., Zhou, S., 2011. Nuclear and chloroplast SSR markers in *Paeonia delavayi* (Paeoniaceae) and cross-species amplification in *P. ludlowii*. Am. J. Bot. 98, e346–e348.

Table S4. Summary of genetic diversity statistics, neutrality tests and mismatch distribution analyses in *Paeonia* subsect. *Delavayanae*. Number of sequences (*N*), polymorphic sites (*S*), number of unique haplotypes (*h*), haplotype diversity (H_d), nucleotide diversity (π), average number of nucleotide difference (*k*). SD = standard desviation. Significance of neutrality parameters were tested by coalescent analyses with their significance (ns, no significant). (R_2), Ramos-Onsins and Rozas's index, (HRI), Harpending's raggedness index.

Group	*N*	*S*	*h*	H_d (SD)	π (SD) $\times 10^{-3}$	*k*	Tajima's *D*	Fu & Li's *D**	Fu & Li's *F**	Fu's F_S	R_2	HRI
P. delavayi + *P. ludlowii*	159	22	14	0.90 (± 0.5 × 10^{-4})	2.08 (± 0.06)	5.57	1.19 ns	1,81 ns	1.88 ns	2.95 ns	0.13 ns	0,07 ns
P. delavayi	137	18	13	0.90 (± 0.7 × 10^{-4})	1.86 (± 0.06)	4.98	1.43 ns	1.69 ns	1.90 ns	2.42 ns	0.14 ns	0.05 ns
P. delavayi (Sichuan + Yunnan)	126	18	13	0.91 (± 0.007)	1.83 (± 0.07)	4.91	1.32 ns	1.69 ns	1.85 ns	2.13 ns	0.14 ns	0.05 ns
DY-WEI1	8	1	2	0.43 (± 0.028)	0.16 (± 0.06)	0.43	0.33 ns	0.89 ns	0.83 ns	0.54 ns	0.21 ns	0.20 ns
DY-LIJ	9	2	3	0.67 (± 0.110)	0.29 (± 0.07)	0.78	0.20 ns	–0.22 ns	–0.14 ns	–0.11 ns	0.21 ns	0.26 ns

Table S5. Numerical results from phylogenetic analyses of each independent plastid DNA region and concatenated sequences in *Paeonia* subsect. *Delavayanae*.

Dataset	*psbA-trnH*	*rps16-trnQ*	*ndhF*	*ndhC-trnV(UAC)*	Concatenated sequences
Nº sequences	18	18	18	18	18
Total characters	372	1131	616	626	2745
Variable characters (%)	5 (1.34)	19 (1.68)	16 (2.60)	16 (2.56)	56 (2.04)
Parsimony informative characters	4	8	12	16	30
No. of steps	16	13	21	6	42
No. of trees	6	6	33	2	38
Consistence index (CI)	0.33	0.62	0.75	1.00	0.78
Retention index (RI)	0.00	0.67	0.88	1.00	0.84
Homoplasy index (HI)	0.67	0.38	0.25	0.00	0.22
Model of evolution	F81+G	GTR+G	GTR+G	F81	

Table S6. Mean recent migration rates (*m*) among the studied populations of *Paeonia* subsect. *Delavayanae* estimated from nine nSSR data using the BayesAss program. Values on the diagonal (underlined) are the proportions of individuals in each generation that are not migrants. Simulations in BayesAss show that in instances where there is no information in the data, the mean *m* and 95% confidence interval for datasets of 17 populations are 0.0105 and 0.0000–0.0933, respectively; values in bold are the *m* rates that are informative.

Populations	DS-LIT	DS-MUL	DS-XIA	DT-BOM1	DT-BOM2	DT-NYI	DY-DAL	DY-DEQ	DY-KUN	DY-LIJ	DY-WEI1	DY-WEI2	DY-XIG	L-MAI1	L-MAI2	L-MAI3	L-MAI4
DS-LIT	0.6867	0.0062	0.0055	0.0064	0.0058	0.0066	0.0060	0.0058	0.0054	0.0066	**0.2233**	0.0061	0.0057	0.0059	0.0062	0.0060	0.0060
DS-MUL	0.0013	0.9806	0.0012	0.0014	0.0012	0.0011	0.0011	0.0012	0.0013	0.0015	0.0015	0.0011	0.0009	0.0012	0.0014	0.0009	0.0012
DS-XIA	0.0096	**0.1659**	0.6935	0.0102	0.0091	0.0090	0.0101	0.0096	0.0091	0.0093	0.0093	0.0089	0.0095	0.0089	0.0088	0.0092	0.0100
DT-BOM1	0.0035	0.0030	0.0027	0.9548	0.0026	0.0028	0.0025	0.0027	0.0026	0.0028	0.0030	0.0023	0.0033	0.0036	0.0025	0.0026	0.0028
DT-BOM2	0.0141	0.0145	0.0146	0.0391	0.7489	0.0141	0.0135	0.0136	0.0141	0.0133	0.0134	0.0148	0.0135	0.0148	0.0141	0.0148	0.0148
DT-NYI	0.0141	0.0143	0.0152	0.0665	0.0132	0.7219	0.0136	0.0134	0.0137	0.0145	0.0136	0.0142	0.0151	0.0148	0.0138	0.0134	0.0148
DY-DAL	0.0011	0.0013	0.0011	0.0014	0.0015	0.0011	0.9798	0.0012	0.0012	0.0013	0.0014	0.0012	0.0012	0.0011	0.0015	0.0013	0.0013
DY-DEQ	0.0011	0.0013	0.0013	0.0012	0.0014	0.0013	0.0012	0.9804	0.0012	0.0012	0.0012	0.0011	0.0013	0.0012	0.0012	0.0012	0.0014
DY-KUN	0.0013	0.0012	0.0013	0.0013	0.0013	0.0014	0.0014	0.0010	0.9799	0.0011	0.0011	0.0012	0.0012	0.0014	0.0013	0.0011	0.0016
DY-LIJ	0.0099	0.0479	0.0100	0.0096	0.0091	0.0094	0.0094	0.0102	0.0105	0.6983	0.0095	0.0096	**0.1190**	0.0095	0.0088	0.0097	0.0096
DY-WEI1	0.0019	0.0021	0.0019	0.0020	0.0020	0.0021	0.0022	0.0020	0.0019	0.0017	0.9678	0.0020	0.0020	0.0023	0.0021	0.0019	0.0021
DY-WEI2	0.0033	0.0026	0.0027	0.0029	0.0031	0.0030	0.0037	0.0038	0.0035	0.0040	0.0035	0.9489	0.0033	0.0030	0.0034	0.0029	0.0023
DY-XIG	0.0011	0.0010	0.0013	0.0012	0.0010	0.0014	0.0010	0.0015	0.0014	0.0011	0.0012	0.0011	0.9804	0.0014	0.0014	0.0011	0.0012
L-MAI1	0.0018	0.0015	0.0016	0.0019	0.0020	0.0017	0.0016	0.0017	0.0019	0.0015	0.0015	0.0018	0.0017	0.9727	0.0020	0.0016	0.0016
L-MAI2	0.0136	0.0140	0.0139	0.0129	0.0128	0.0132	0.0139	0.0129	0.0115	0.0122	0.0127	0.0124	0.0126	0.0990	0.7076	0.0120	0.0129
L-MAI3	0.0137	0.0150	0.0146	0.0140	0.0134	0.0144	0.0144	0.0152	0.0148	0.0142	0.0133	0.0145	0.0141	0.0382	0.0133	0.7484	0.0144
L-MAI4	0.0135	0.0131	0.0149	0.0148	0.0146	0.0131	0.0147	0.0130	0.0132	0.0145	0.0152	0.0148	0.0138	0.0646	0.0150	0.0148	0.7224

Table S7. Predicted potential distribution of *Paeonia* subsect. *Delavayanae* for all general circulation models used in this study.

Model	Predicted area (km^2)	Difference respect to present (km^2 and %)	Overlap with present (km^2 and %)	Mean elevation (m)
P. delavayi				
Present	273,749	—	—	3160
LGM-CCSM	152,514	–121,235 (–44.29)	129,386 (47.26)	2824
LGM-MIROC	72,759	–200,990 (–73.42)	63,164 (23.07)	3052
LGM-MPI	193,679	–80,070 (–29.25)	151,635 (55.39)	2754
Average LGM	*139,651*	*–134,098 (–48.99)*	*114,728 (41.91)*	*2877*
P. ludlowii				
Present	32,791	—	—	3116
LGM-CCSM	117,116	+84,325 (+257.16)	31,515 (96.11)	3143
LGM-MIROC	31,529	–1262 (–3.85)	17,943 (54.72)	2828
LGM-MPI	20,677	–12,114 (–36.94)	273 (0.83)	1281
Average LGM	*56,441*	*+23,649 (+72.12)*	*16,577 (50.55)*	*2417*
P. delavayi + *P. ludlowii*				
Present	248,243	—	—	2950
LGM-CCSM	116,221	–132,022 (–53.18)	95,293 (38.39)	2875
LGM-MIROC	59,071	–189,172 (–76.20)	49,473 (19.93)	2996
LGM-MPI	159,494	–88,749 (–35.75)	113,026 (45.53)	2727
Average LGM	*111,595*	*–136,647 (–55.05)*	*85,931 (34.62)*	*2866*